3D Printing for Geoscience: Fundamental Research, Education, and Applications for the Petroleum Industry

Sergey Ishutov[1,2], Dawn Jobe[1], Shuo Zhang[1], Miguel Gonzalez[1], Susan M. Agar[1], Franciszek J. Hasiuk[2], Francesca Watson[3], Sebastian Geiger[3], Eric Mackay[3], Richard Chalaturnyk[4]

1. Aramco Research Center, Houston
2. Department of Geological and Atmospheric Sciences, Iowa State University
3. Institute of Petroleum Engineering, Heriot-Watt University
4. Department of Civil and Environmental Engineering, University of Alberta

Manuscript for Geohorizons, AAPG Bulletin

Abstract

3D printing provides a fast, cost-effective way to produce and replicate complicated designs with minimal flaws and little material waste. Early use of 3D printing for engineering applications in the petroleum industry has stimulated further adoption by geoscience researchers and educators. Recent progress in geoscience is signified by capabilities that translate digital rock models into 3D-printed "rock proxies." With a variety of material and geometric scaling options, 3D printing of near- identical rock proxies provides a method to conduct repeatable laboratory experiments without destroying natural rock samples. Rock-proxy experiments can potentially validate numerical simulations and complement existing laboratory measurements on changes of rock properties over geologic timescale. A review of published research from academic, government, and industry contributions indicates a growing community of rock-proxy experimentalists. 3D-printing techniques are being applied to fundamental research in the areas of multi-phase fluid flow and reactive transport, geomechanics, physical properties, geomorphology, and paleontology. Further opportunities for geoscience research are discussed. Applications in education include teaching models of terrains, fossils, and crystals. The integration of digital datasets with 3D-printed geomorphologies supports communication for both societal and technical objectives. Broad benefits that could be realized from centralized 3D printing facilities are also discussed.

INTRODUCTION

The phrase "3D printer" has entered the popular lexicon as "a 21st Century technology that turns digital designs into 3D physical objects, whenever you want them at low cost." Many forward thinkers and visionaries in industry, academia, and government see value in 3D printing. 3D-printed objects ("3D prints") complement digital presentations and visualization tools, providing a physical representation of 3D geometries that enhances communication. While digital models can be viewed only on a screen, a 3D print can be experienced with all the senses: it can be viewed, manipulated, smelled, tasted, and more importantly experimented with in the laboratory. 3D printing provides a way to quickly test new concepts and can generate different objects over a wide range of scales with high accuracy and repeatability. These "rapid prototyping" capabilities provide cost-effective approaches that are shaping the future of manufacturing. 3D printing is expected to drive new innovations, initiating a decentralized industrial revolution, and to impact business by up to $550 billion per year by 2025 (Cohen et al., 2014). Benefits of 3D printing for engineering applications in the petroleum industry are already being realized. Flexible options for design and a variety of materials have supported 3D printing of drill-bits and tools such as a drill sleeve with built-in flow monitoring, a fine mesh in a downhole fluid analysis tool, a hydraulic manifold and a hydraulic line for subsea well stimulations and acid treatments (Jacobs, 2016).

Reduced costs of 3D printers, open-source software, and free access to digital model repositories are opening new avenues for many fields of research. Among these, geoscience is poised to use 3D printing to bridge the gap between computational and experimental analyses. Recognizing this opportunity, this paper provides an overview, limitations, and potential applications of 3D-printing technology, as applied to geoscience research and education as well

as the petroleum industry.

3D PRINTING METHODS

Similar to traditional laser- or inkjet "2D" printers, 3D printers construct images in layers (a form of additive manufacturing; Burns, 1993). While a 2D printer prints a single, very thin layer of ink, a 3D printer builds a stack of layers in one or more materials. Therefore, we use the term "printing" in the rest of the paper to represent "3D printing." All 3D printing methods evolved from stereolithography (SLA) technology patented by C. Hull in 1986. In SLA, a digital 3D geometry (e.g., Computer-Aided Design (CAD) file) is transformed into a physical object, layer-by-layer (Berman, 2012). Prior to 3D printing physical objects, digital models are "sliced" to create the layer templates. Printing specifications set by the user include the thickness of each slice, the vertical and horizontal dimensions, and the print speed. Printed objects often require post-processing, such as ultraviolet (UV) light curing or removal of support material (that holds the internal porous structure and external elements during printing to avoid deformation or damage of intricate designs).

3D printing methods that use a layer-by-layer technique differ by power source, resolution, precision, accuracy, build volume, materials, and price (Table 1) and can be grouped as follows: (1) photopolymerization (SLA, Digital Light Processing (DLP)) that involves UV or light curing layers of the liquid material on a build platform; (2) extrusion (Fused Deposition Modeling (FDM) and Fused Filament Fabrication (FFF), Inkjet (Material jet or Polyjet), Direct Ink Writing and Direct Laser Writing (DIW and DLW)) that jets a liquid or melted material through the print-head nozzle; (3) fusion (Selective Laser Sintering and Melting (SLS and SLM), Electron Beam Melting and Welding (EBM andEBW), Laser Engineered Net Shaping (LENS)) involving

a-laser energy source that fuses powder material to build fully dense objects; and (4) deposition (Laminated Object Manufacturing (LOM), Selective Deposition Lamination (SDL), Binder Jetting) that involves layering of the powder material cured by glue or lamination of solid layers cut by laser or tungsten blade to create surface roughness (Gibson et al., 2014).

FROM DIGITAL MODELS TO 3D-PRINTED ROCK PROXIES

The convergence of 3D printing with methods that digitally capture the 3D structure of a rock on multiple scales has created new opportunities for geoscience research. Academic researchers and government agencies have been at the vanguard (Choi et al., 2011; Hasiuk et al., 2015; Ishutov et al., 2015; Martinez et al., 2015; Osinga et al., 2015; Head and Vanorio et al., 2016; Jiang et al., 2016a; Watson et al., 2016; Hasiuk et al., 2017). A primary research focus is the reproduction of the internal structure of a rock (e.g., pore architecture, fractures) with controlled solid and surface properties for the purposes of experimentation (e.g., wettability). We refer to these reproductions as "rock proxies." The scale of rock proxies can vary over the orders of magnitude: from nanometer-size features to the size of the 3D printer's build volume. In addition, a combination of multiple proxies could produce larger-scale modules (e.g., 3D printing facies of a reservoir rock). Rock proxies are generated from digital models and provide a novel way to link numerical modeling and laboratory experiments (Figure 1). Digital models are commonly defined by multi-scale geoscience data (e.g., tomographic, microscopic, core, well logs, seismic, and outcrop data) which are then translated for printing via: (1) CAD files for volume or shape generated models; (2) deterministic inputs (e.g., directly from tomography or microscopy); or (3) stochastic inputs (e.g., from pore sizes and distributions).

Rock proxies can support the quantitative assessment of rock properties and processes such

as fluid transport (e.g., porosity, permeability, wettability, migration), electrical response (e.g., resistivity), mechanical behavior (e.g., Young's modulus, Poisson's ratio), chemical interactions (e.g., reactive transport), and acoustic signatures (e.g., sonic velocity). The substitution of rock proxies for natural rock samples in laboratory experiments provides a way to repeat measurements with systematic changes in the rock texture or environment. Repetition of physical experiments (e.g., tomographic imaging of flow and transport in porous media) today is limited by the fact that they are routinely conducted in a destructive manner or on a small number of samples (Blunt et al., 2013; Bultreys et al., 2016) and can involve chemical reactions which trigger precipitation and dissolution inside pore space (Luquot et al., 2014; Menke et al., 2016). Destructive testing has the limitation that comparative analysis of fluid behavior can only be performed if multiple near-identical rock samples are available; this is usually not the case because two rock samples are never identical, even for a homogeneous rock. 3D printing thus provides the opportunity to perform destructive testing on near-identical pore networks that are representative of the natural rocks.

Capabilities and Limitations for 3D Printing of Rock Proxies

Advanced applications of rock proxies require a close match between the natural rocks to be replicated and their 3D-printed proxies. Future research will need to minimize errors associated with printing, artifacts, and inaccurate geometries that may impact experimental results. We identify four primary challenges for 3D printing of rock proxies: (1) achieving appropriate imaging resolution for data capture; (2) achieving adequate precision and accuracy in 3D-printed proxies of intricate internal geometry in natural rocks, including pore throats (the smallest flow elements in the pore system); (3) developing materials that respond in a similar manner to rocks

(e.g., chemical, geomechanical); and (4) developing multi-material and multi-fluid 3D printing methods to represent a natural fluid-rock system.

Image Resolution: Accurate replication of a natural rock depends on image resolution, image data processing, and the method and material used in 3D printing (Ishutov and Hasiuk, 2014). The resolution of rock images continues to improve, with capabilities to capture very fine-scale features of rocks, such as nanopores in shales (Nelson, 2009). However, analysis of digital rock models is challenged by two factors: (1) a given image pixel or voxel size may obscure the boundaries between rock features making edge identification difficult; and (2) file size and computational intensity increase with improved image resolution (Idowu et al., 2014). These limitations tend to drive the selection of small sample sizes that may be unrepresentative of rock properties at a larger scale, making it difficult to integrate plug- and core-scale rock properties with well log, seismic, and outcrop data (Andrä et al., 2013; Guice et al., 2014).

Proxy Accuracy and Precision: The accuracy of a printed proxy is impacted by the 3D printing methods, materials used, printing parameters (e.g., layer thickness), post-processing methods (e.g., UV curing, glue impregnation, airflow), image resolution, dimensions of digital models, and the degree of scaling of the digital model to the 3D-printed object (Dimitrov et al., 2006). The maximum precision and resolution depend on the mechanical processes associated with each 3D printing method. For example, in the extrusion method the resolution is determined by the precision of the print-head movement in the X-Y direction and the physico-chemical properties of the build material; in the photopolymerization method, the resolution is primarily controlled by the size of the laser spot or resolution of the light projector; and in fusion and deposition methods, the resolution depends on the size of powder particles and their layering pattern on the build platform. Currently, the DIW and DLW methods provide the highest resolution, precision,

and accuracy among all 3D printing methods (~1 micron for solid features; Table 1). However, no studies to our knowledge have yet validated individual grain or pore sizes at this resolution. To overcome resolution and accuracy challenges, the digitally captured rock fabric may need to be rescaled for a given experiment. Rescaling is an increase or a decrease in the digital model size to build a proxy according to the 3D printer's resolution and, or build volume or to accommodate experimental conditions. This rescaling will impact measurements of rock properties (e.g., permeability) and will need to be factored into the interpretation of experimental results. Given recent progress improving 3D printing resolution and introduction of automated precision systems in 3D printers (Gao et al., 2015; Brommer et al., 2016; Duarte et al., 2016), we anticipate that improvements in 3D-printing capabilities will achieve a closer representation of the true internal geometry of natural rock (on a sub-micron scale). In addition, development of calibration or standard models is necessary for quantification of printing resolution and identification of artifacts. These models will allow us to determine how accurately a 3D-printed proxy reproduces a digital model in terms of geometry (e.g., size and surfaces) and properties (e.g., porosity and density).

Material Properties: 3D printers can use a range of build materials (plastic, metals, resin, ceramics, mineral powder, paper, biomaterials). While no currently available material is capable of replicating all the relevant properties of natural rock simultaneously, different materials impact the resolution achievable in a rock proxy. At present, materials can be selected for a given model based on their suitability to be used to investigate an individual property separately (e.g., flow, electrical, acoustic, mechanical).

The chemical properties of mineral powders (e.g., gypsum, silica, and calcite) used to 3D print rock proxies are close to natural rock, but the mechanical properties of proxies are often

weaker (with Uniaxial Compressive Strength (UCS) < 3 MPa (435 psi); Farzadi et al., 2015; Fereshtenejad and Song, 2016) and have artifact porosity between powder particles. Moreover, these proxies require infiltrant (glue) impregnation in post-processing that can lead to erroneous microporosity values as measured via gas or mercury porosimetry. Gypsum material can be suitable for pore systems with large pore throats (>500 microns; Ishutov et al., 2016), which have a minimal risk of either becoming clogged by powder particles or trapping remaining infiltrant droplets.

Plastic materials used in fusion or material jetting technologies can change the dimensions of 3D-printed proxies due to shrinkage or expansion. Some plastics (e.g., acrylonitrile butadiene styrene (ABS), polylactic acid (PLA)) have inadequate strength for destructive mechanical or core-flood experiments because they can break or flow at lower stresses (e.g., <40 MPa (5,800 psi); Jiang and Zhao, 2015). Differences in the flow properties between 3D-printed samples and the original rocks can also result from the clogging of the pore space by the residual plastic during or after printing. Thermoplastics can be used for studies of more homogeneous pore systems to avoid warping and deformation of solid objects and the associated changes in pore volumes.

Metals are one of the stiffest 3D printing materials that can currently be used in studies of mechanical properties of rock proxies. While they offer potential for use in electrical and acoustic experiments, the prices of 3D printers that print metal are not yet at the commodity level. In addition, the resolution of these 3D printers (50 microns; Gao et al., 2015) is not yet high enough to 3D print porous rocks without rescaling.

Resin is an organic material with physical and chemical properties that can be adjusted by mixing different resin components, by adding pigments, and by varying post-processing

procedures. The material supports fast 3D printing; for example, a core plug (one inch (2.54 cm) in diameter and two inches (5.08 cm) in length) can be printed in 4 hours. When hardened, the resin can reach a stiffness of ~86 MPa (12,500 psi) (Ju et al., 2014). The resolution (200 microns for the smallest feature; Head and Vanorio, 2016) of resin-based 3D printers is relatively high when compared to other methods used to reproduce the pore systems of homogeneous rocks (Table 1). The wettability of resin-based proxies can be altered by using a chemical polish, vapor deposition, or silanization (Martinez et al., 2015; Zhao et al., 2016). Clear materials can be used for the development of optically transparent devices to help real-time process imaging, especially in models with areas that are difficult to access by conventional polishing methods.

3D Printer Methods. Beyond the challenges of proxy precision, accuracy, and materials, 3D printers still need further development to meet the specifications of rock proxies. With the expiration of two key 3D printing patents in 2014 (Deckard, 1989; Bourell et al., 1990), 3D printers can now be designed in a broad range of configurations to achieve higher resolution, faster printing speed, and controlled physical and chemical properties of materials. For example, SLA and inkjet 3D printers can be used to manufacture features that are less than one micron in size by using new infrared laser polymerization (Vaezi et al., 2013; Skylar-Scott et al., 2016). The novel CLIP (continuous liquid interface production) method that uses oxygen at the bottom of the resin pool after each UV light pass resolves the issue of liquid material trapped in the voids of the 3D-printed object (Tumbleston et al., 2015). The interdrop or interparticle porosity in the 3D printing material can be reduced or even eliminated with adjustable drop shape in nanofluidic printers (Meister et al., 2009). These advances will enable more accurate 3D printing of pore shapes, improving measurements of flow properties. In addition, future development of binder jet methods may involve an introduction of a binder that can change the wettability of

powder grains during or after the 3D printing process, similar to methods of wettability control that are used in microfluidic devices (Gerami et al., 2016). Knowing contact angles between solid and liquid constituents in the 3D-printed proxy will help to predict relative permeability in multi-phase flow experiments. Multi-material 3D printers can be widely applied in manufacturing of natural rock proxies with heterogeneous textures. Multi-material printing requires a synthesis of two or more 3D printing methods, but the advantage is that physico-chemical properties for each material can be designed independently (e.g., metal powder and alloy ink; Jakus et al., 2015). Another area of development for the majority of 3D printing methods is post-processing. More efficient ways to remove support material in inkjet, binder jet (powder-based), and photopolymerization 3D printers are needed to enable accurate printing of fine details and features, such as channels, specifically in microfluidic devices. Incomplete removal of such support material can result in erroneous experimental measurements.

FUNDAMENTAL RESEARCH, EDUCATION, AND APPLICATIONS

The following section builds on recent advances for 3D printing of rock proxies to discuss how this approach can benefit geoscience research as well as broader applications for geoscience education and communication. We provide examples of how 3D printing helps in studying natural rock properties and processes associated with their changes at microscopic and macroscopic scales over geologic time. Recommendations on the improvement of existing methods of 3D printing proxies outlined in this section can also lead to generation of novel ideas for broadening the applications of 3D printing in the petroleum industry.

Microfluidics and Flow in Geological Systems

"Microfluidics" is a set of technologies used in the fabrication of micro-devices for fluid analysis in the physical sciences (Gunda et al., 2011). The term has evolved to include all non-trivial devices for fluid-flow experiments and flow phenomena that occur at micron scales (Whitesides and Stroock, 2001; Stone et al., 2004). The field has highlighted new physical phenomena at micrometer scales that are characteristically different from those at larger scales (Lenormand et al., 1988; Tabeling, 2005). Scaling laws are introduced when a system is reduced in size from macroscopic- to the microscopic scale. For instance, surface forces and volumetric forces, such as gravity, scale differently. Surface forces are important in fluid investigations, including wetting, adhesion, friction, and lubrication (e.g., coatings, biotechnology, super hydrophobic surfaces, and micro-electro-mechanical systems). In a rock, wetting and the boundary layers at the fluid-rock and fluid-fluid contacts strongly influence fluid flow over geologic and production timescales. Furthermore, chemical reactions (e.g., during diagenesis or fluid injection) increase the flow complexity by changing the interfacial forces. Large-scale, 3D-printed fluidic systems (rock proxies), that mimic natural rocks and include micro-channel structures with tunable surface chemistry, can help to deepen our understanding of multi-scale flow (Figure 2).

One of the first implementations of 3D printing in microfluidics (McDonald and Whitesides, 2002) used printed molds to create a polydimethylsiloxane replica of a 3D network of channels. Using this technique, Wu et al. (2003) created a chaotic advective mixer by generating braided and out of plane networks of 3D channels. These early 3D-printed devices had a surface roughness of several microns. This scale of roughness can reduce the integrity of seals between surfaces. However, consumer-grade SLA printers today can achieve a sub-micron surface roughness (Comina et al., 2014). More recently, Bhargava et al. (2014) constructed a toolbox of

3D-printed, discrete microfluidic elements and interconnects for a modular 3D-microfluidics platform. They constructed microfluidic circuits in which each discrete element had well catalogued properties and for which pressure-flow relationships were obtained by network analysis (as in an electrical circuit). Other examples of 3D-printed microfluidic devices include membranes (Femmer et al., 2014), devices with integrated valves (Rogers et al., 2015), scaffolds for tissue engineering (Hollister, 2005) and Li-ion microbatteries (Sun et al., 2013).

In the petroleum industry, microfluidic devices (commonly referred to as micromodels) date back to the 1950s (e.g., Chatenever and Calhoun, 1952). They have been heavily used to investigate the displacement of oil by an immiscible fluid and other two-and three-phase flow phenomena. Micromodel studies have provided insights to percolative processes, relative permeability of water and oil, and the Saffman-Taylor instability (Saffman and Taylor, 1958), all of which affect oil recovery. While not technically micromodels, Hele-Shaw cells (Bischofberger et al., 2014) and packed glass beads still provide significant insight to fluid flow processes (Murison et al., 2014). The first micro-devices used in the petroleum industry were rudimentary, with simple pore structures fabricated in glass. The pore structures were generated either by etching or by adding repetitive elements such as small spheres (Karadimitriou and Hassanizadeh, 2012).

To achieve a closer 3D representation of natural rocks, Park et al. (2015) used SLA to create "2.5D" rock micromodels (in which the same 2D geometry is repeated in the third dimension). Song et al. (2014) developed methods to fabricate microfluidic channels in natural calcite to add more realistic surface physics to their micromodel similar to carbonate rocks. Similarly, Mugele et al. (2016) used oxidized silicon wafers with adsorbed nanoparticle clays to fabricate micro-channels in an attempt to simulate the typical composition of a sandstone. They were able to tune

the wettability of the micro-channels to gain insight to the fundamental aspects of low-salinity water flooding. In contrast, Zhao et al. (2016) used a photocurable polymer with soft imprint lithography to systematically alter the wettability of microfluidic samples and analyze fluid-fluid displacement efficiency as a function of wettability.

Experiments have also been used to explore the feasibility of 3D printing to model soil macropore networks. Bacher et al. (2014) used X-ray computed tomography to digitize the macropore structure which was then 3D-printed using SLA in various polymeric materials. The morphologies of soil pore-network structures have been replicated at high resolution (tens of microns) to study fungal growth in soil microcosms (Otten et al., 2012) and the impact of micro-heterogeneities on soil-water dynamics (Dal Ferro et al., 2015).

Progress in microfluidic models combined with pore-scale imaging and 3D printing provide a foundation for future geoscience research. This research can advance flow experiments that are used typically to study physico-chemical interactions between fluids and rocks (McDougall and Mackay, 1998; Bultreys et al., 2016). In multi-phase flow studies, such as enhanced oil recovery or carbon capture and storage, the replication of wettabilities will be crucial (Ryazanov et al., 2014; Zhang et al., 2016a). A better understanding of fluid trapping and mobilization could be achieved through *a priori* knowledge of wettability distribution as defined in a model design. Similarly, the generation of rock proxies with realistic chemical properties can improve our insights into reactive transport processes. This could be accomplished by altering chemical composition at specific sites (e.g., replicated grain surfaces) in a rock proxy.

3D printing can be also used to investigate the scaling relationships of flow processes (e.g., changes in permeability). Unknown pore-scale heterogeneity prevents comparisons of results from pore-scale and Darcy-scale flow experiments on the same natural rock. With 3D printing, it

is possible to make a rock proxy with known pore geometries (Figure 2). This can provide repeated models that are at or below the scale of the representative elementary volume. The combination of many such models can be used to construct a larger (and heterogeneous) model to improve and test rescaling methods for both chemically inert and reactive transport problems (Li et al., 2008).

For advances in core-flood and reactive transport experiments, we envisage an integrated experimental design in which parts of the experimental rig are included in the rock proxy. Integration of a core holder and fluid inlet and outlet lines with the rock proxy would allow fluids to be introduced at various locations instead of just at the edges. This configuration would reduce edge effects, such as capillary end effects arising due to the differences between pore sizes in the core and the width of channels in the end piece platen or gaps due to the roughness of the end of the core. It would also enable the study of more complicated mixing scenarios, for example the injection of incompatible brines through multiple but distinct channels to ensure first mixing occurs in the porous medium rather than in the inlet lines.

Embedded sensors in 3D-printed rock proxies would strengthen understanding of the chemical and physical processes and greatly improve the validation of numerical simulations. Leigh et al. (2012) demonstrated that sensors could be created and integrated with 3D printing to measure capacitance and flexure. Rock proxies could also be printed with in-situ fiber optic sensors (Maier et al., 2013) enabling parameters such as pressure, temperature or chemical composition to be monitored internally. Lin et al. (2016) demonstrated that smart microgels can be used as sensors to detect real-time chemical changes in microfluidic platforms.

Some 3D printing materials also offer a way to explore the impacts of physical properties on flow (e.g., due to microporosity in carbonate rocks with wide pore size distributions; Pak et al.,

2016). Binder Jetting Powder Deposition (BJD) printers use fine powder (calcium hemisulfate, calcium polyphosphate, or hydroxyapatite) that is held together with an organic binder (Butscher et al., 2012). The 3D-printed solid, however, retains micropores between the individual powder grains. As such, the solid yet microporous printed powder can mimic micrite in carbonates and may support a method to systematically control the amount and distribution of micropores within a rock proxy. This approach is similar to the use of BJD 3D printers in bioengineering to generate synthetic porous bone tissue scaffolds (Pilliar et al., 2001; Farzadi et al., 2015). Representations of microporosity in rock proxies highlight an opportunity to study multi-scale interactions between macro-scale pore- and fracture- and microporous systems.

Significant advances have been made to numerically model single- and multi-phase flow displacement processes through realistic pore geometries (Blunt, 2001; Blunt et al., 2013; Meakin and Tartakovsky, 2009; Joekar-Niasar et al., 2013). However, there remains uncertainty when defining parameters for numerical simulations, for instance in relation to surface wettability and contact angles (Sorbie and Skauge, 2012). 3D printing experiments can help to validate the results of numerical simulations and more rigorously quantify displacement processes through joint interpretation of experimental and numerical results.

Several of the approaches discussed above (e.g., embedded sensors, multi-scale experiments, validation of numerical models) are applicable to experimentation in other geoscience disciplines (e.g., geomechanics, geophysics) that are discussed in the sections that follow.

Macroscopic Physical Rock Properties

Macroscopic properties are defined by bulk measurements that represent a spatially averaged quantity beyond the microscopic scales of the pore dimensions. These properties include, but are

not limited to, flow-, electrical- (resistivity), acoustic- (P and S wave velocities, sonic, ultrasonic), and magnetic- (e.g., Nuclear Magnetic Resonance (NMR)) properties. Electrical properties of the subsurface have been key for oil exploration since the inception of resistivity logging and the development of Archie's empirical law to calculate water saturation in a sandstone (Archie, 1942). Therefore, the dielectric response of the mineral-fluid system in the porous matrix of rocks has been a subject of intense research. Acoustic properties of a Newtonian fluid imbibed in an elastic porous matrix can be described by Biot's theory (Biot, 1956). This formalism has been applied in several areas of geoscience, including the determination of fluid saturations in rocks (Murphy et al., 1986) and acoustic propagation in fractured rocks (White, 1975; Müller et al., 2010). Insight into these fluid and rock properties has helped to strengthen interpretations of acoustic logs (Cheng, et al., 1982). NMR has been applied via wireline logging (Akkurt et al., 2009) and laboratory measurements in core samples (Lonnes et al., 2003). Information from NMR measurements is useful to obtain physical and chemical properties such as porosity and fluid saturation (Timur, 1969) and viscosity (Nicot et al., 2007), and wettability (Freedman et al., 2003; Odusina et al., 2011).

Models that relate rock and fluid properties (stress state and saturation state, fluid density, and viscosity) to the macro-scale properties (flow, electrical, acoustic, magnetism) are key for interpretations in the subsurface. For example, modeling the effects of fluid saturation on seismic velocity is used to ascertain the influence of pore fluids on acoustic signatures. Gassmann's equations (Berryman, 1999), which are essentially the lower frequency limit of Biot's (1956) more general equations of motion for poroelastic materials, are most widely used to calculate seismic velocity changes resulting from different fluid saturations in reservoirs. However, many of the basic assumptions in Gassmann's equations are invalid for some common reservoir rocks

and fluids (Han and Batzle, 2004). Laboratory experiments play a vital role in understanding the basic rules needed to inform both simulations and modeling. As much as we strive to achieve controlled conditions in laboratory experiments, it is extremely difficult to be complexly prescriptive for all of the possible responses of heterogeneous rocks and fluids. This level of complexity requires a different approach.

With 3D-printed rock proxies, the experimental procedure can be improved substantially. The uncertainties in measuring density, porosity, and bulk modulus can be greatly reduced by the use of homogeneous materials with consistent compositions to avoid the complications that arise from multiple mineral constituents. By printing multiple copies of the same rock proxy, the effects of different fluid saturations on velocity can be isolated (Figure 3).

Huang et al. (2014) used 3D printing to create 4% porosity models of rocks in ABS thermoplastic. They created fractured media proxies which increased the porosity by 20% and studied changes in ultrasound propagation in fractured and unfractured media that were air or water saturated. Head and Vanorio (2016) linked experimental diagenesis, multi-scale imaging techniques, and 3D-printed proxies of varying carbonate microstructures to study the evolution of bulk porosity and permeability. They were able to mimic the process of compaction and dissolution, producing porosity-permeability trends that were quantitatively distinct from each other. Such results allow researchers to determine which factors underpin the theoretical predictions of porosity-permeability evolution during diagenesis that have previously been derived using numerical pore-scale modelling (van der Land et al., 2013). These are only a few of the exploratory efforts in the use of 3D printing to investigate macroscopic rock properties. 3D printing will continue to improve rapidly in utility and contribute to our ability to access delicate samples and to test the impact of microstructural alteration on bulk physical properties in the

laboratory in a highly consistent, repeatable manner. The following section on multiphase flow discusses novel ideas that build on this emerging technology to implement new experimental approaches.

The constitutive relations that define how multi-phase flow properties (e.g., the bulk porosity, permeability, capillary pressure, and relative permeabilities) change due to mineral precipitation (Zhang et al., 2016b), have not been validated experimentally. Constant salt precipitation during core-flood experiments makes it difficult to achieve the steady-state flow that is required to measure multi-phase flow properties. 3D printing will allow experiments to be paused and examined: the pore structure modified by salt precipitation can be imaged at discrete time points. Then each image can be printed separately and used to establish the capillary pressure and relative permeability curves. This unprecedented approach decouples the measurement of multi-phase flow properties from the continuous salt precipitation in a core-flood experiment. The validated constitutive relations will have significant impacts on the prediction of formation damage caused by salt precipitation (Zhang and Liu, 2016).

The dependence of permeability on effective stress is important for the petroleum industry, especially in natural gas recovery from tight shale reservoirs which can show high stress sensitivity. Zheng et al. (2015) developed a series of theoretical models for the relationship between permeability and effective stress based on the concept of the Two-Part Hooke's Model (TPHM). The TPHM conceptualizes an intact rock into a hard part which corresponds to the rock matrix and a stress sensitive soft part which corresponds to the microcracks in the rock. The model has been validated against experimental data on natural rock samples. The volume ratio of the two parts is used as a tuning parameter to fit experimental data, but cannot be isolated in natural rocks. With 3D printing, the volume and distribution of micro-cracks can be precisely

controlled and used to quantify the impact of the volume ratio on stress-dependent permeability. Instead of being a tunable parameter, the volume ratio would then be a known value. Experiments with systematically designed rock proxies can be used to test whether the TPHM provides an appropriate model to explain the observed stress-permeability trends.

Geomechanics

3D printing can be used to substitute rock proxies in experimental analysis of rock deformation and failure. A key advantage is the ability to control rock textures and the generation of near-identical samples with homogeneous properties so that experiments can be repeated with the same "rock" while systematically changing the experimental conditions. 3D printing also enables the systematic inclusion of various heterogeneities, such as microcracks, stylolites, joints, and vugs across multiple, near-identical test specimens. By knowing and controlling inter-sample variability in terms of porosity, fracture networks, grain size distribution, and density distribution, 3D printing of geomaterials provides a valuable tool to validate numerical models, develop scaling laws and constitutive relationships, quantify the degree of influence of pore geometry, fracture network characteristics, and structural heterogeneity on macroscopic properties (Figure 4). This also becomes critical for understanding the impact of deformation on fundamental fluid-flow processes such as relative permeability or capillary pressure and enables a new generation of reservoir-geomechanical experiments to be designed for validating coupled processes embedded in simulation models.

Reports of geomechanical experiments based on 3D printed rock or soil proxies are growing in the literature. Jiang and Zhao (2015) used PLA and FDM to produce test specimens for preliminary compressive shear and tensile strength experiments. The study highlighted the

limitations of PLA as a material for experimentation, demonstrated the influence of 3D-printed structure specimen response and identified the need to use a more suitable rock-like material for printing. Jiang et al (2016a) utilized both PLA and FDM and powder-binder systems to print specimens as substitutes for natural rock specimens in experimental deformation studies. These experiments confirmed the inapplicability of PLA for producing rock-like specimens and highlighted that the compressive strengths of powder-binder printed specimens of less than 10 MPa (1,500 psi) are below those of most rocks. Osinga et al. (2015) printed directly with sand (D_{50} of 148 μm) using BJD and reported compressive strengths approaching 20 MPa (2,900 psi) and a cemented grain structure that reflects natural sandstone (Figure 4). In a preliminary effort to visualize the internal structure and stress distribution of rocks, Ju et al. (2014) describe methods to capture fracture geometries in natural coal rock and the stress concentrations associated with them. By "freezing" rock stresses and using photoelastic effects they were able to visualize stress concentrations and local stress gradients around discrete fractures during mechanical testing and compare these images with numerical solutions. Jiang et al. (2016b) pursued a method to model the surfaces of natural joints as a way to reduce experimental errors originating from the use of natural samples in shear tests. In their study of soil mechanical behavior, Matsumura and Muzutani (2015) used X-ray CT scans of gravel to print replicas and compare their mechanical responses with those of natural samples. While there were differences in the mechanical responses between natural (stiffer) and replicated samples, modifications to the replicas provided a demonstration of the way that particle arrangements impact load-displacement curves.

The details of the 3D printing process also make a difference to the properties of the systems: in printing the porosity structure of natural bone, Fazardi et al. (2015) found that delay times (50

to 500 ms) between printing each layer introduced differences in compressive strength, toughness and tangent modulus as well as higher dimensional accuracy. While exploring the impact of layer orientation on sample strength for the purposes of optimizing bone strength, Vlasea et al. (2015) found the weakest orientations for compressive strength to result from layering perpendicular to, or at 45^{o} to the compression direction, while layering parallel to the compression direction created the strongest samples. The same approach could be used to control the strength of samples relative to the maximum loading direction in deformation experiments on textured rock proxies. Phase composition and macroporosity were found to be more influential than pore geometries on the strength of calcium phosphate scaffolds used as bone substitutes (Schumacher et al., 2010). New techniques, such as topological optimization in tissue engineering to meet design requirements (e.g., stiffness), offer further ways to condition material properties by ensuring that tissue scaffold stiffness remains the same until porosity reaches a certain value (Almeida and Bartolo, 2010). Nevertheless, as yet, there are no standards for mechanical testing of 3D printed materials which, in particular, require careful consideration of anisotropy in mechanical properties introduced as the result of most 3D printing methods (Roberson et al., 2015).

Clearly, further advances in 3D printing for geomechanics will require an expanded research effort to create materials and textures suitable to represent different rock types and minerals. Improvements in printing resolution can support the inclusion of specific flaws and heterogeneities in a rock proxy for investigations of geologic controls on strain localization. Similar methods have been used to design populations of fractures within a rock proxy. With this approach we envisage experiments that measure variations in acoustic properties with increasing complexity of fracture arrays and networks that might be designed in discrete fracture network

models (Huang et al., 2015). In addition to printing multi-phase or multi-material models, new materials will need to be able to withstand subsurface conditions for high temperature and pressure experiments. Developments in biomedical fields also point to more sophisticated possibilities for experimentation: 3D printing of bone scaffolds is beginning to incorporate controlled chemistry and interconnected porosity, and capabilities for site-specific growth factor and drug delivery (Bose et al., 2013). With these advances, future rock deformation experiments might include controls on fluid content location and chemistry to investigate coupled deformation and reactive transport as well as embedment of sensors (similar to examples discussed for fluid flow studies above) directly within the test specimens. 3D printing of rock proxies can serve as the foundation for the next generation of experimental investigations of multi-scale, multi-physics reservoir geomechanical processes. Explicit control over the heterogeneous nature of test specimens will help to reduce uncertainties regarding the delineation of geological features over a wide range of length scales, to represent these features appropriately in reservoir geomechanical simulations, and to quantify the impact of deformations on flow, as well as their impacts on evolving multi-phase fluid distributions. In summary, with suitable technological advances in hardware and materials, 3D printing has significant potential to deliver new fundamental knowledge in geomechanics.

Geomorphology and Paleontology

3D printing can be used to generate rescaled representations of the Earth's surface, subsurface morphologies, and relief on planetary bodies. 3D-printed geomorphic representations complement computer-generated models and provide important tools for communication, teaching, and scientific research (Peterson et al., 2015; Hasiuk et al., 2017). While geoscientists

have strived to perform their work in the digital realm, considerable value still resides in the physical representation of geologic systems. Previously, translation of digital data (such as Digital Elevation Models (DEMs)) into physical models was achieved through molding and sculpting, limiting the level of detail and materials employed and requiring significant labor. Initially, 3D printing was identified as a tool to generate the molds for raised relief maps (Ahmed et al., 2005; Higgins, 2010). Today, 3D printing offers a rapid method to generate physical objects from digital files, enabling easier visual inspection and the use of a wider range of materials (Horowitz and Schultz, 2012). Hasiuk et al. (2017) document the development of a direct digital manufacturing platform that simplifies the process of generating 3D-printable terrain models to selecting a polygon in a web browser's map.

Initiatives to combine 3D printing with other technologies have realized further advances. The potential to link spatial analysis tools such as ArcGIS™ (ESRI software) to 3D printing can serve to integrate multi-disciplinary geologic information accurately on printed surfaces (e.g., superimposing RADAR, SONAR, and satellite imagery). The feasibility of this approach has already been demonstrated in the context of urban planning (Ghawana and Zlatanova, 2013). In the development of a collaborative land navigation system, Li et al. (2014) combined augmented reality with 3D printing to facilitate interactions between an explorer and a remote overseer.

3D printing of morphologies also has value to geoscience research. In the experiments of rock-breakdown processes (weathering and erosion of rock masses that form sedimentary debris), Bourke et al. (2008) used 3D printing to replicate the morphology of rock blocks for testing under various environmental conditions. Although the experiments were limited to morphology and did not replicate the internal structure or residual stresses, they generated new insights to the persistence of fluvial features subject to weathering (Figure 5). In another

example, DEMs of gravel-bed morphologies were captured through water and air to define 3D-printed models of river beds as substrates in hydraulic experiments (Bertin et al., 2014). This study showed that the 3D printed model provided a dense and accurate set of check-point data that could be used to assess the quality of the DEMs (as opposed to lower precision survey check points).

Description, classification, and preservation of paleontological specimens has also benefited from 3D printing. In a study of the remains of a dwarf elephant, Mitsopoulou et al. (2015), scanned the original bones via laser to capture the surface morphology and combined them in 3D-printed proxies. 3D-printed microfossils developed from tomographic imaging combined with 3D-PDFs have now supported an improved taxonomy (Mahmood et al., 2014). Balanoff and Rowe (2007) used tomographic scanning to digitally extract and 3D print the embryonic skeleton of an elephant bird egg without breaking the eggshell. Paleoichnological research has also benefited from the ability of 3D printers to enlarge natural objects (Hasiotis et al., 2011). Such approaches create an opportunity to compare and study morphologies without risk to the original specimen. 3D printing will facilitate the democratization of access to research collections by allowing non-experts to interact with high-quality specimens, either digital or 3D-printed, without a trip to a distant museum or specialized training. For example, the British Geological Survey is overseeing the 3D scanning of all type fossils in British collections for distribution through the GB3D website (www.3d-fossils.ac.uk). Overall, the ability of 3D printing to accurately duplicate geologic morphologies is opening up new associations between physical models, digital data, and tools that support the communication of integrated information, rigorous quantification for research, and fast, complete archiving.

Education and Communication

It is natural that geoscientists, who work regularly with 3D data, might embrace 3D printing to communicate their interpretations to other geoscientists, students, stakeholders, and the broader public (Hasiuk, 2014). For those who are not used to thinking spatially, 3D-printed models are easier to understand than a 2D representation (such as a map) because physical models are less of an abstraction. Printed models preserve the 3D nature of the original data (including the internal structure) rather than relying on other features (e.g., contour lines, map symbols) to convey the third dimension. As shown in Figure 6, geoscientists have used 3D printing to make terrain models (e.g., Horowitz and Schultz, 2014; Hasiuk et al., 2017), fossil specimens (e.g., Hasiotis et al., 2011; Rahman et al., 2012; Mahmood et al., 2014), crystallographic models (Casas and Estop, 2015), geological structures (Reyes et al., 2008), and pore networks (Otten et al., 2012; Ishutov et al., 2015). Models printed in plastic are often more rugged than plaster or wooden counterparts. While 3D topographic maps have existed for decades, they are typically only available for charismatic locales (e.g., the Grand Canyon, USA). Now educators can print any terrain for which elevation data exist (Hasiuk et al., 2017). In addition, the generation of libraries of physical objects makes areas of geoscience more accessible to people in general, including the visually handicapped. The promise of 3D printing for educational purposes has been recently reinforced by energy industry sponsorship of the Fab Foundation (www.fabfoundation.org) to open 3D printing laboratories (Fab Labs) across the United States of America.

In addition to education, 3D printing has value for the communication of geoscience to generalist audiences, for example to convey changes associated with urban development and environmental policies, to support legal arguments, and to provide general knowledge of natural heritage in national parks. In museums the “third wave industrial revolution” is supporting the

replication and restoration of artifacts that facilitates sharing exhibits among archiving institutions (Short, 2015). 3D printing has been used in the restoration of museum collections. Scanning of preserved fossils and modeling of missing parts enabled the University of Michigan Museum of Paleontology to assemble a mastodon skeleton for display (Fisher et al., 2012). A missing femur was replicated by 3D scanning, digital mirroring, and printing the opposite femur. Similarly, the Smithsonian National Museum of Natural History 3D-scanned an entire fossil of a whale skeleton in Chile for 3D printing in the USA. The digital model was used to reduce the size of the skeleton so it would fit in the exhibit space (Reese, 2014; Byers and Woo, 2015).

A recent Italian initiative illustrates the value of 3D printing for communicating geology to industry stakeholders (DeFilippis et al., 2015). The project involves 3D printing reservoir models created from seismic and well data, representing colored rock layers and faults that help to make geological concepts and data more accessible (DeFilippis et al., 2015). Such approaches support collaborations among colleagues from diverse disciplines: a geologist and engineer can plan well placements based on reservoir geometry and local topography using the same 3D-printed proxy that complements digital geological data; a manager can use the same model to discuss developments with local governments and communities. Reducing the cognitive burden of understanding 3D concepts will facilitate more efficient communication and will reduce errors or misunderstandings.

Development of Central Facilities

3D printers enable low-volume production and mass-customization in an economical manner. Obtaining access to a low-cost 3D printer is straightforward but rarely will it automatically meet the specific needs for scientific research or commercial objectives. Advanced 3D printers that

can handle large volume- (meter- or foot-scale), multi-material- or extremely high resolution prints are commonly beyond the budgets of potential users (well over $100,000; Table 1). A leasing option can be more cost-effective than a full purchase given the rapid evolutions in 3D printing technology. Laboratory space, however, would still be needed. Central (or mobile) facilities for 3D printing minimize upfront investment for low-volume users and can provide access to the latest equipment and materials, support co-developments, and handle printing requests submitted online.

3D printers have been accessible via community- or university libraries for several years (Britton, 2012; Free, 2012; Scalfani and Sahib, 2013; Colegrove, 2014). Dedicated 3D printing facilities are also now established and growing in several US universities and government laboratories (Fidan and Ghani, 2007; Choi et al., 2011; Budig et al., 2013; Raviv et al., 2014; Tibbits et al., 2014; Torrado Perez et al., 2014; Bechtold, 2015). Sandia National Laboratories offer rapid prototyping services for small businesses as part of America Makes, the US national business accelerator for additive manufacturing. A similar public-private partnership underpins rapid prototyping services via China's National Laboratories for 3D Printing (Simon, 2015). As of 2015, there were over twenty online platforms to support 3D printing services in a digital market place (e.g., Lan, 2009; Rayna et al., 2015; Tapley et el., 2016).

In the context of geoscience research and education, centralized 3D printing facilities and exchanges within their user communities are likely to accelerate the development of specialized methods for 3D printing of geologic geometries and textures. Those who have considered printing their "reservoir" (Agar et al., 2013; Ishutov and Hasiuk, 2014) might eventually submit geocellular models online to a facility that not only prints reservoir models to a specified scale but also runs scientific experiments on large models in the same location. In addition, cloud

computing services could numerically simulate properties of the digital model online. Williams (2013) recognized the opportunity to generate shared file collections so that educators could print samples locally or remotely for use with courses, citing their variably scaled models of the Mariana Trench and San Andreas Fault as part of a tectonic plate boundary collection. The National Institutes of Health "3D Print Exchange" provides an example of how such digital collections might work (www.3dprint.nih.gov) through an interactive website for sharing biomedical 3D-print files and modeling tutorials and educational material.

The potential to disrupt manufacturing sites and supply chains with new and relocatable 3D printing "factories" is widely recognized (Waller and Fawcett, 2014). With this shift, come numerous concerns related to intellectual property that have spawned new business models. Some 3D printing companies have adopted a selectively open innovation strategy by which user-generated content complements proprietary hardware and software (West and Kuk, 2016). However, the petroleum industry is still in the early stages of developing systems to protect 3D printing intellectual property while supporting collaboration and innovation (Eldred and Basiliere, 2015). Whether so-called direct digital manufacturing (DDM) actually disrupts rather than complements the manufacturing economy has yet to be seen (Sasson and Johnson, 2016), but the opportunities for co-creation between inventors and 3D printing centers or firms is already changing paths to innovation (Rayna et al., 2015).

A central facility would ensure high-quality research instrumentation for 3D printing. If it encompassed the multiplicity of 3D printing methods and materials (Pham and Gault, 1998), it would not only be extremely expensive but also require an abundance of support personnel. More feasible would be a facility that generates proxies at a specific scale (overall dimension of the 3D-printed model) and resolution (smallest observable feature). For the petroleum industry,

such a facility might initially aim for the core-plug scale with pore-scale resolution. Future developments could move to larger scales (e.g., whole core, mini-reservoir) and, or higher resolutions and a wider range of materials.

Centralized facilities could support the 3D printing of large (tens of meters or hundreds of feet) artificial reservoir models as a means to interrogate the near-wellbore environment. The "reservoir print" could be manufactured with and without a wellbore to test the effects of drilling on subsequent well performance, the use of completion tools and logging tool responses. Again, sensors could be embedded into a large model as it is 3D-printed for internal monitoring. It might be possible for such large models to calibrate seismic responses to known reservoir architecture. The construction of multi-scale geologic features over seven or more orders of magnitude clearly presents a challenge. However, the feasibility of large model development is supported by the fact that 3D printers are capable of printing house-size structures (Kenney, 2016) by using cementitious materials, fiber-reinforced plastic, and glass fiber-reinforced gypsum as feedstock (Sevenson, 2015).

A centralized facility for printing rock proxies should also have the capability to verify the accuracy of 3D-printed objects. Just as standards for mechanical testing were discussed above, a repository could serve to establish standards for collecting and reporting metadata from all the steps in 3D model making and printing. A repository of examples with different 3D printing capabilities could be used to coordinate inter-laboratory comparisons of 3D printing accuracy and precision.

CONCLUSIONS

Based on our direct experience and the examples discussed above, 3D printing is positioned for

an expanded role in geoscience research and education as well as more broadly in the petroleum industry. Building on early progress that can now translate digital rock models into rock proxies, 3D printing methods have the potential to support diverse investigations of properties and processes in rock proxies over multiple scales. These methods could be used to complement and validate numerical simulations. Currently 3D printing of rock proxies is limited by several factors, particularly the precision achievable for internal geometries as well as a lack of suitable materials for rock replication. Nevertheless, cost reductions in hardware are making high-resolution and multi-material 3D printers more readily accessible, supporting an expanded community of geoscience experimentalists in 3D printing. Potential and growing areas of applications for research include multi-phase fluid flow, reactive transport, geomechanical behaviors, and physical rock properties. Large, multi-disciplinary experiments might also be supported at scales suitable for near-wellbore or reservoir flow unit investigations. Beyond geoscience research, 3D printing complements digital visualization for the communication of concepts and ideas whether these are in the context of education, community, or industry. A 3D printing future for the geosciences is likely to be strengthened by a growing number of central facilities. These facilities would not only provide 3D printing services, but also support the development of open repositories of digital models and standards for verification of proxy accuracy and precision while stimulating multi-disciplinary connections around geoscience questions.

REFERENCES

Agar, S. M., S. Geiger, P. Leonide, J. Lamarche, G. Bertotti, O. Gosselin, G. Hampson, M. Jackson, G. Jones, J. Kenter, S. Matthai, J. Neilson, L. Pyrak-Nolte, and F. Whitaker,

2013, Fundamental controls on flow in carbonates – summary of an AAPG-SPE-SEG Hedberg Conference, Saint Cyr-sur-mer: AAPG Bulletin, v. 97, p. 533-552, doi: 10.1306/12171212229.

Ahmed, K., D. McCallum, D., and D. F. Sheldon, 2005, Multi-phase micro-drop interaction in inkjet printing of 3D structures for tactile maps: Modern Physics Letters, v. 19, no. 28-29, p. 1699-1702, doi: 10.1142/S0217984905010256.

Akkurt, R., H. N. Bachman, C. C. Minh, C. Flaum, J. LaVigne, R. Leveridge, R. Carmona, S. Crary, E. Decoster, N. Heaton, N., and M. D. Hurlimann, 2009, Nuclear magnetic resonance comes out of its shell: Oilfield Review, v. 20, no. 4, p. 4-23.

Almeida, H. de A., and P. J. da S. Bartolo, 2010, Virtual topological optimization of scaffolds for rapid prototyping: Medical Engineering and Physics, v. 32, no. 7, p. 775-782, doi: 10.1016/j.medengphy.2010.05.001.

Andrä, H., N. Combaret, J. Dvorkin, E. Glatt, J. Han, M. Kabel, Y. Keehm, F. Krzikalla, M. Lee, C. Madonna, M. Marsh, T. Mukerji, E. H. Saenger, R. Sain, N. Saxena, N., S. Ricker, A. Wiegmann, and X. Zhan, 2013, Digital rock physics benchmarks—Part II: Computing effective properties: Computers and Geosciences, v. 50, p. 33–43, doi: 10.1016/j.cageo.2012.09.008.

Archie, G. E., 1942, The electrical resistivity log as an aid in determining some reservoir characteristics: Transactions of the AIME, v. 146, no. 1, p. 54-62, doi: 10.2118/942054-G.

Bacher, M., A. Schwen, and J. Koestel, 2014, Three-dimensional printing of macropore networks of an undisturbed soil sample: Vadose Zone Journal, v. 14, no. 2, doi: 10.2136/vzj2014.08.0111.

Balanoff, A. M., and T. B. Rowe, 2007, Osteological Description of an Embryonic Skeleton of the Extinct Elephant Bird, *Aepyornis* (Palaeognathae, Ratitae): Journal of Vertebrate Paleontology, Memoir 9, v. 27, p. 1-54, doi: 10.1671/0272-4634.

Barco, J. L., G. Cuenca-Bescós, V. Sauque, J. I. Canudo, A. Moros, R. Perruca, and J. Lorente, 2010, Using digitization and rapid prototyping technologies to replicate an urus cranium: The Geological Curator, v. 9, no. 3, p. 199-206.

Bechtold, S., 2015, 3D printing and the intellectual property system: World Intellectual Property Organization, Economic-Research Working Paper, 27 p.

Berman, B., 2012, 3D printing: the new industrial revolution: Business Horizons, v. 55, no. 2, p. 155-162.

Berryman, J., 1999, Origin of Gassmann's equations: Geophysics, v. 64, no. 5, p.1627-1528, doi: 10.1190/1.1444667.

Bertin, S., H. Friedrich, P. Delmas, E. Chan, and G. Gimel'farb, 2014, DEM quality assessment with a 3D printed gravel bed applied to stereophotogrammetry: The Photogrammetric Record, v. 146, p. 241-264, doi: 10.1111/phor.12061.

Bhargava, K. C., B. Thompson, and N. Malmstadt, 2014, Discrete elements of 3D microfluidics: Proceedings of the National Academy of Sciences of the United States of America, v. 111, no. 42, p. 15013-15018, doi: 10.1073/pnas.1414764111.

Biot, M. A., 1956, Theory of Propagation of Elastic Waves in a Fluid-Saturated Porous Solid. I. Low-Frequency Range: Journal of Acoustic Society of America, v. 28, no. 168, doi: 10.1121/1.1908239.

Bischofberger, I., R. Ramachandran, and S. R. Nagel, 2014, An island of stability in a sea of fingers: emergent large-scale features of the viscous flow instability: Soft Matter, v. 11,

no. 37, p. 7428-7432, doi: 10.1039/C5SM00943J.

Blunt, M. J., 2001, Flow in porous media—pore-network models and multi-phase flow: Current opinion in colloid and interface science, v. 6, no. 3, p. 197-207, doi: 10.1016/S1359-0294(01)00084-X.

Blunt, M. J., B. Bijeljic, H. Dong, O. Gharbi, S. Iglauer, P. Mostaghimi, A. Paluszny, and C. Pentland, 2013, Pore-scale imaging and modeling: Advances in Water Resources, v. 51, p. 197-216, doi: 10.1016/j.advwatres.2012.03.003.

Bonyar, A., Santha, H., Ring, B., Varga, M., Kovacs, J. G., and G. Harsanyi, 2010, 3D rapid prototyping technology (RPT) as a powerful tool in microfluidic development: Procedia Engineering, v. 5, p. 291-294, doi: 10.1016/j.proeng.2010.09.105.

Bourell, D. L., J. H. L. Marcus, J. W. Barlow, J. J. Beaman, and C. R. Deckard, 1990, Multiple material systems for selective beam sintering: US Patent 4944817A, filed September 5, 1989, and issued July 31, 1990, 15 p.

Bourke, M., H. Viles, J. Nicoli, P. Lyew-Ayee, R. Ghent, and J. Holmund, 2008, Innovative applications of laser scanning and rapid prototype printing to rock breakdown experiments: Earth Surface Processes and Landforms, v. 33, p. 1614-1621, doi: 10.1002/esp.1631.

Bose, S., S. Vahabzadeh, and A. Bandyopadhyay, 2013, Bone tissue engineering using 3D printing: Materials Today, v. 16, p. 497-504, doi: 10.1016/j.mattod.2013.11.017.

Britton, L., 2012, A fabulous laboratory: Public Libraries, v. 52, p. 30-33.

Brommer, D. B., T. Giesa, D. I., Spivak, and M. J. Buehler, 2016, Categorical prototyping: incorporating molecular mechanisms into 3D printing: Nanotechnology, v. 27, no. 2, p. 1-8, doi: 10.1088/0957-4484/27/2/024002.

Budig, M., M. Kohler, and F. Gramazio, 2013, The tectonics of 3D-printed architecture: Gazette Future Cities Lab, no. 19.

Bultreys, T., W. De Boever, and V. Cnudde, 2016, Imaging and image-based fluid transport modeling at the pore scale in geological materials: A practical introduction to the current state-of-the-art: Earth-Science Reviews, v. 155, p. 93-128, doi: 10.1016/j.earscirev.2016.02.001.

Burns, M., 1993, Automated fabrication: improving productivity in manufacturing: Prentice Hall, Englewood Cliffs, 369 p.

Butscher, A., M. Bohner, C. Roth, A. Ernstberger, R. Heuberger, N. Doebelin, P. R. von Rohr, and R. Muller, 2012, Printability of calcium phosphate powders for three-dimensional printing of tissue engineering scaffolds: Acta Biomaterialia, v. 8, p. 373-385, doi: 10.1016/j.actbio.2011.08.027.

Byers, C., and A. Woo, 2015, 3D data visualization: The advantages of volume graphics and big data to support geologic interpretation: AAPG-SEG Interpretation, v. 3, no. 3, p. SX29-SX39, doi: 10.1190/INT-2014-0257.1.

Camisa, J. A., V. Verma, D. O. Marler, and A. Madlinder, 2014, Additive Manufacturing and 3D Printing for Oil and Gas - Transformative Potential and Technology Constraints: Proceedings of the Twenty-fourth International Ocean and Polar Engineering Conference Busan, Korea, ISOPE-I-14-595.

Casas, L., and E. Estop, 2015, Virtual and printed 3D models for teaching crystal symmetry and point groups: Journal of Chemical Education, 92, p. 1338-1343, doi: 10.1021/acs.jchemed.5b00147.

Chatenever, A., and J. C. Calhoun, 1952, Visual examinations of fluid behavior in porous media:

Part I: Transactions of Metallurgical Society of AIME, v. 195, p. 149-156.

Cheng, C. H., M. N. Toksöz, and M. E. Willis, 1982, Determination of in situ attenuation from full waveform acoustic logs: Journal of Geophysical Research: Solid Earth, v. 87, no. B7, p. 5477-5484, doi: 10.1029/JB087iB07p05477.

Choi, J. W., R. Quintana, and R. Wicker, 2011, Fabrication and characterization of embedded horizontal micro-channels using line-scan stereolithography: Rapid Prototyping Journal, v. 17, no. 5, p. 351-361, doi: 10.1108/13552541111156478.

Cohen, D., M. Sargeant, and K. Somers, 2014, 3D printing takes shape: McKinsey Quarterly, http://www.mckinsey.com/business-functions/operations/our-insights/3D-printing-takes-shape, accessed March, 2016.

Colegrove, P., 2014, Making it real: 3D printing as a library service: EDUCAUSE Review, http://er.educause.edu/articles/2014/10/making-it-real-3d-printing-as-a-library-service, accessed March, 2016.

Comina, G., A. Suska, and D. Filippini, 2014, Low cost lab-on-a-chip prototyping with a consumer grade 3D printer: Lab on a Chip, v. 14, no. 16, p. 2978-2982, doi: 10.1039/C4LC00394B.

Dal Ferro, N., A. G. Strozzi, C. Duwig, P. Delmas, P. Charrier, and F. Morari, 2015, Application of smoothed particle hydrodynamics (SPH) and pore morphologic model to predict saturated water conductivity from X-ray CT imaging in a silty loam Cambisol: Geoderma, v. 255–256, p. 27–34, doi: 10.1016/j.geoderma.2015.04.019.

Deckard, C. R., 1989, Method and apparatus for producing parts by selective sintering: US Patent 4863538A, filed October 17, 1986, and issued September 5, 1989, 12 p.

DeFilippis, P., M. Grechi, F. Napoli, F. Quattrocchi, R. Santoleri, and M. Melatti, 2015, A new

experience for public-awareness towards public-acceptance in Exploration and Production: 3D - real reservoir representation: 12th Offshore Mediterranean Conference and Exhibition, OMC-2015-476.

Dimitrov, D., K. Schreve, and N. De Beer, 2006, Advances in three-dimensional printing – state of the art and future prospectives: Rapid Prototyping Journal, v. 12, no. 3, p. 136-147, doi: 10.1108/13552540610670717.

Duarte, L. C., T. C. de Carvalho, E. O. Lobo-Junior, P. V. Abdelnur, B. G. Vaz, and W. K. T. Coltro, 2016, 3D printing of microfluidic devices for paper-assisted direct spray ionization mass spectrometry: Analytical Methods, v. 8, p. 496-503, doi: 10.1039/c5ay03074a.

Eldred, M., and P. Basiliere, 2015, Impact of 3D printing for oil and gas industry IT leaders: Gartner, G00280151, https://www.gartner.com/doc/3178318/impact-d-printing-oil-gas, accessed July, 2016.

Farzadi, A., V. Waran, M. Solati-Hashjin, and Z. A. A. Rahman, 2015, Effect of layer printing delay on mechanical properties and dimensional accuracy of 3D printer porous prototypes in bone tissue engineering: Ceramics International, v. 41, no. 7, p. 8320-8330, doi: 10.1016/j.ceramint.2015.03.004.

Femmer, T., F. Carstensen, and M. Wessling, 2014, A membrane stirrer for product recovery and substrate feeding: Biotechnology and Bioengineering, v. 112, no. 2, p. 331-338, doi: 10.1002/bit.25448.

Fereshtenejad, S., and J.-J. Song, 2016, Fundamental Study on Applicability of Powder-Based 3D Printer for Physical Modeling in Rock Mechanics: Rock Mechanics and Rock Engineering, v. 49, no. 6, p. 2065-2074, doi: 10.1007/s00603-015-0904-x.

Fidan, I., and N. Ghani, 2007, Acquisition steps of a remotely accessible rapid prototyping laboratory: International Journal of Computer Applications in Technology, v. 30, no. 4, p. 266-272, doi: 10.1504/IJCAT.2007.017238.

Fisher, D., S. O'Grady, S. Hamm, B. Lyons, and L. Schumann, 2012, Mending a Broken Mastodon with Rapid Prototyping and 3D Scanning: UM3D Lab, http://um3d.dc.umich.edu/blmending-a-broken-mastodon-with-rapid-prototyping-and-3d-scanning/, accessed July, 2016.

Free, D., 2012, University of Nevada-Reno Library offers 3D printing: College and Research Libraries News, v. 73, no. 8, p. 454-457.

Freedman, R., N. Heaton, M. Flaum, G. J. Hirasaki, C. Flaum, and M. Hürlimann, 2003, Wettability, saturation, and viscosity from NMR measurements: SPE Journal, v. 8, no. 4, p. 317-327, doi: 10.2118/87340-PA.

Gao, W., Y. Zhang, D. Ramanujan, K. Ramani, Y. Chen, C. B. Williams, C. C. L. Wang, Y. C. Shin, S. Zhang, S., and P. D. Zavattieri, 2015, The status, challenges, and future of additive manufacturing in engineering: Computer-Aided Design, v. 69, p. 65-89, doi: 10.1016/j.cad.2015.04.001.

Gerami, A., P. Mostaghimi, R. T. Armstrong, A. Zamani, and M. E. Warkiani, 2016, A microfluidic framework for studying relative permeability in coal: International Journal of Coal Geology, v. 159, p. 183-193, doi: 10.1016/j.coal.2016.04.002.

Ghawana, T., and S. Zlatanova, 2013, 3D printing for urban planning: a physical enhancement of spatial perspective: Urban and Regional Data Management UDMS Annual.

Gibson, I., D. Rosen, and B. Stucker, 2014, Additive Manufacturing Technologies: New York, Springer, 498 p.

Gunda, N. S. K., B. Bera, N. K. Karadimitriou, S. K. Mitra, and S. M. Hassanizadeh, 2011, Reservoir-on-a-Chip (ROC): A new paradigm in reservoir engineering: Lab on a Chip, no.11, p. 3785-3792, doi: 10.1039/C1LC20556K.

Han, D.-h., and M. L. Batzle, 2004, Gassmann's equation and fluid-saturation effects on seismic velocities: Geophysics, v. 69, no. 2, p. 398-405, doi: 10.1190/1.1707059.

Hasiotis, S. T., D. R. Hirmas, B. F. Platt, and J. Reynolds, 2011, New frontiers in ichnology using MLT and rapid prototyping for 3D analysis, printing, and sharing of modern and ancient traces with other ichnophiles: Geological Society of America Abstracts with Programs, v. 43, p. 81.

Hasiuk, F. J., C. Harding, A. Renner, and E. Winer, 2017, TouchTerrain: A Simple Web-Tool for Creating 3D-Printable Topographic Models: Computers and Geosciences (in press).

Hasiuk F., 2014, Making things geological: 3D printing in the geosciences: GSA Today, v. 24, no. 8, p. 28-29, doi: 10.1130/GSATG211GW.1.

Hasiuk, F., L. J. Florea, and M. C. Sukop, 2015, Three-dimensional printing: transformative technology for experimental groundwater research: Groundwater, v. 54, no. 2, doi: 10.1111/gwat.12394.

Hasiuk, F., and C. Harding, 2016, Touchable topography: 3D printing elevation data and structural models to overcome the issue of scale: Geology Today, v. 32, no. 1, p. 16-20, doi: 10.1111/gto.12125.

Head, D. A., and T. Vanorio, 2016, Effects of changes in rock microstructure on permeability: 3D printing investigation: Geophysical Research Letters, v. 43, doi: 10.1002/2016GL069334.

Higgins, M. H., 2010, Method for manufacturing raised relief maps: US Patent 20100102476

A1, filed October 29, 2008, and issued April 29, 2010, 11 p.

Hollister, S. J., 2005, Porous scaffold design for tissue engineering: Nature materials, v. 4, no. 7, p. 518-524, doi: 10.1038/nmat1421.

Horowitz, S. S., and P. H. Schultz, 2012, Printing space: 3D printing of digital terrain models for enhanced student comprehension and educational outreach: Geological Society of America Annual Meeting and Exposition, v. 44, no. 7, p. 95.

Huang, L., R. Stewart, and N. Dyaur, 2014, Elastic properties of 3D-printed rock models: dry and saturated cracks: American Geophysical Union Fall Meeting, MR11B-4320.

Hull, C. W., 1986, Apparatus for production of three-dimensional objects by stereolithography: US Patent 4575330A, filed August 8, 1994, and issued March 11, 1986, 16 p.

Idowu, N. A., C. Nardi, H. Long, T. Varslot, and P.-E. Øren, 2014, Effects of segmentation and skeletonization algorithms on pore networks and predicted multi-phase-transport properties of reservoir-rock samples: Society of Petroleum Engineers Reservoir Evaluation and Engineering, v. 17, no. 4, p.473-483, doi: 10.2118/166030-PA.

Ishutov S., S. M. Fullmer, A. S. Buono, F. J. Hasiuk, C. Harding, and J. Gray, 2016, Resurrection of a reservoir sandstone from tomographic data using 3D printing: AAPG Bulletin (in press).

Ishutov, S., and F. J. Hasiuk, 2014, 3D printing helps reservoir modeling: American Oil and Gas Reporter, v. 57, no. 12, p. 125-127.

Ishutov, S., F. J. Hasiuk, C. Harding, and J. Gray, 2015, 3D printing sandstone porosity models: Interpretation 3D Visualization, v. 3, no. 3, p. SX49-SX61, doi: 10.1190/INT-2014-0266.1.

Jacobs, T., 2016, 3D printing in the oil field kicks into production mode: Journal of Petroleum

Technology, v. 68, no. 8, p., 30-36.

Jakus, A. E., S. L. Taylor, N. R. Geisendorfer, D. C. Dunand, and R. N. Shah, 2015, Metallic architecture from 3D-printed powder-based liquid links: Advanced Functional Materials, v. 25, no. 45, p. 6985-6995, doi: 10.1002/adfm.201503921.

Jiang, C., and G.-F. Zhao, 2015, A preliminary study of 3D printing on rock mechanics: Rock Mechanics and Rock Engineering, v. 48, no. 3, p. 1041-1050, doi: 10.1007/s00603-014-0612-y.

Jiang, Q., X. Feng, L. Song, Y. Gong, H. Zheng, and J. Cui, 2016a, Modeling rock specimens through 3D printing: tentative experiments and prospects: Acta Mechanica Sinica, v. 32, no. 1, p. 101-111, doi: 10.1007/s10409-015-0524-4.

Jiang, Q., X. Feng, L. Song, Y. Gong, L. Song, S. Ran, and J. Cui, 2016b, Reverse modelling of natural rock joints using 3D scanning and 3D printing: Computers and Geotechnics, v. 73, p. 210-220, doi: 10.1016/j.compgeo.2015.11.020.

Joekar-Niasar, V., F. Doster, R. T. Armstrong, D. Wildenschild, and M. A. Celia, 2013, Trapping and hysteresis in two-phase flow in porous media: A pore-network study: Water Resources Research, v. 49, no. 7, p. 4244-4256, doi: 10.1002/wrcr.20313.

Ju, Y., H. Xie, Z. Zheng, J. Lu, L. Mao, G. Feng, and R. Peng, 2014, Visualization of the complex structure and stress field inside rock by means of 3D printing technology: Chinese Science Bulletin, v. 59, no. 36, p. 5354-5365, doi: 10.1007/s11434-014-0579-9.

Karadimitriou, N. K., and S. M. Hassanizadeh, 2012, A review of micromodels and their use in two-phase flow studies: Vadose Zone Journal, v. 11, no. 3, doi: 10.2136/vzj2011.0072.

Kenney, 2016, Let's print together the first adobe building: WASP Project, http://www.wasproject.it/w/en/stampiamo-insieme-la-prima-casa-di-terra/, accessed July,

2016.

Lan, H., 2009, Web-based rapid prototyping and manufacturing systems: a review: Computers in Industry, v. 60, no. 9, p. 643-656, doi: 10.1016/j.compind.2009.05.003.

Leigh, S. J., R. J. Bradley, C. P. Purssell, D. R. Billson, and D. A. Hutchins, 2012, A simple, low-cost conductive composite material for 3D printing of electronic sensors: PloS one, v. 7, no. 11, doi: 10.1371/journal.pone.0049365.

Lenormand, E., C. Touboul, and C. Zarcone, 1988, Numerical models and experiments on immiscible displacements in porous media: Journal of Fluid Mechanics, v. 189, p. 165-187, doi: 10.1017/S0022112088000953.

Li, L., C. I. Steefel, and L. Yang, 2008, Scale dependence of mineral dissolution rates within single pores and fractures: Geochimica et Cosmochimica Acta, v. 72, no. 2, p. 360-377, doi: 10.1016/j.gca.2007.10.027.

Li, N., E. Sharlin, A. S. Nittala, and M. Costa Sousa, 2014, Shvil: collaborative augmented reality land navigation: Proceedings, Extended Abstracts on Human Factors in Computing Systems, p. 1291-1296, doi: 10.1145/2559206.2581147.

Lin, S., W. Wang, X.-J. Ju, R. Xie, Z. Liu, H.-R. Yu, C. Zhang, and L.-Y. Chu, 2016, Ultrasensitive microchip based on smart microgel for real-time online detection of trace threat analyses: Proceedings of the National Academy of Science, v. 113, no. 8, p. 2023-2028, doi: 10.1073/pnas.1518442113.

Lonnes, S., A. Guzman-Garcia, and R. Holland, 2003, NMR petrophysical predictions on cores: 44th Annual Logging Symposium, Society of Petrophysicists and Well-Log Analysts, SPWLA-2003DDD.

Luquot, L., T. S. Roetting, and J. Carrera, 2014, Characterization of flow parameters and

evidence of pore clogging during limestone dissolution experiments: Water Resources Research, v. 50, no. 8, p. 6305-6321, doi: 10.1002/2013WR015193.

Mahmood, S., B. M. Hussaini, F. Hasiuk, D. N. Schmidt, and E. Thomas, 2014, Microfossils in 3D: scans, 3D-pdf, 3D-printing: GSA Annual Meeting.

Maier, R. R. J., W. N. MacPherson, J. Barton, M. Carne, M. Swan, J. N. Sharma, S. K. Futter, D. A. Knox, B. J. S. Jones, and S. McCulloch, 2013, Embedded fibre optic sensors within additive layer manufactured components: IEEE Sensors Journal, v. 13, no. 3, p. 969-979, doi: 1109/JSEN.2012.2226574.

Martinez, M. J., H. Yoon, and T. A. Dewers. 2015, 3D printing and digital rock physics for geomaterials: AGU Fall Meeting, MR43A-01.

Matsumura, S., and T. Mizutani, 2015, 3D printing of soil structure for evaluation of mechanical behavior: 14th International Congress for Stereology and Image Analysis, 4 p.

McDonald, J. C., and G. M. Whitesides, 2002, Poly(dimethylsiloxane) as a material for fabricating microfluidic devices: Accounts of Chemical Research, v. 35, no. 7, p. 491-499, doi: 10.1021/ar010110q.

McDougall, S. R., and E. J., Mackay, 1998, The impact of pressure-dependent interfacial tension and buoyancy forces upon pressure depletion in virgin hydrocarbon reservoirs: Chemical Engineering Research and Design, v. 76, no. A5, p. 553-561, doi: 10.1205/026387698525234.

Meakin, P., and A. M. Tartakovsky, 2009, Modeling and simulation of pore-scale multi-phase fluid flow and reactive transport in fractured and porous media: Reviews of Geophysics, v. 47, no. 3, doi: 10.1029/2008RG000263.

Meister, A., M. Gabi, P. Behr, P. Studer, J. Vörös, P. Niedermann, J. Bitterli, J. Polesel-

Maris, M. Liley, H. Heinzelmann, and T. Zambelli, 2009, FluidFM: Combining Atomic Force Microscopy and Nanofluidics in a Universal Liquid Delivery System for Single Cell Applications and Beyond: Nanoscience Letters, *v.* 9, no. 6, p. 2501–2507, doi: 10.1021/nl901384x.

Menke, H. P., M. G. Andrew, M. J. Blunt, and B. Bijeljic, 2016, Reservoir condition imaging of reactive transport in heterogeneous carbonates using fast synchrotron tomography—Effect of initial pore structure and flow conditions: Chemical Geology, v. 428, p. 15-26, doi: 10.1016/j.chemgeo.2016.02.030.

Mitsopoulou, V., D. Michailidis, E. Theodorous, S. Isidorou, S. Roussiakis, T. Vasilopoulos, S. Polydoras, G. Kaisarlis, V. Spitas, E. Stathapoulou, C. Provatidis, and G. Theodorou, 2015, Digitizing, modelling and 3D printing of skeletal digital models of Palaeoloxodon tiliensis (Tilos, Dodecanese, Greece): Quaternary International, v. 379, p. 4-13, doi: 10.1016/j.quaint.2015.06.068.

Mugele, F., I. Siretanu, N. Kumar, B. Bera, L. Wang, R. de Ruiter, A. Maestro, M. Duits, D. van den Ende, and I. Collins, 2016, Insights from ion adsorption and contact-angle alteration at mineral surfaces for low-salinity waterflooding: SPE Journal, v. 21, no. 4, p. 1204-1213, doi: 10.2118/169143-PA.

Müller, T. M., B. Gurevich, and M, Lebedev, 2010, Seismic wave attenuation and dispersion resulting from wave-induced flow in porous rocks—A review: Geophysics, v. 75, no. 5, p. 75A147-75A164, doi: 10.1190/1.3463417.

Murison, J., B. Semin, J.-C. Baret, S. Herminghaus, M. Schroeter, and M. Brinkmann, 2014, Wetting heterogeneities in porous media control flow dissipation: Physical Review Applied, v. 2, doi: 10.1103/PhysRevApplied.2.034002.

Murphy III, W. F., K. W. Winkler, and R. L. Kleinberg, 1986, Acoustic relaxation in sedimentary rocks: Dependence on grain contacts and fluid saturation: Geophysics, v. 51, no. 3, p. 757-766, doi: 10.1190/1.1442128.

Nelson, P. H., 2009, Pore-throat sizes in sandstones, tight sandstones, and shales: AAPG Bulletin, v. 93, no. 3, p. 329–340, doi: 10.1306/10240808059.

Nicot, B., M. Fleury, and J. Leblond, 2007, Improvement of viscosity prediction using NMR relaxation: 48th Annual Logging Symposium, Society of Petrophysicists and Well-Log Analysts, SPWLA-2007-U.

Odusina, E. O., C. H. Sondergeld, and C. S. Rai, 2011, NMR study of shale wettability: Canadian Unconventional Resources Conference, Society of Petroleum Engineers, doi: 10.2118/147371-MS.

Osinga, S., G. Zambrano-Narvaez, and R. J. Chalaturnyk, 2015, Study of geomechanical properties of 3D-printed sandstone analogue, ARMA Conference, Paper 2015-547.

Otten, W., R. Pajor, S. Schmidt, and R. E. Falconer, 2012, Combining X-ray CT and 3D printing technology to produce microcosms with replicable, complex pore geometries: Soil Biology and Biochemistry, v. 5, p. 53-55, doi: 10.1016/j.soilbio.2012.04.008.

Pak, T., I. B. Butler, S. Geiger, M. I. J. van Dijke, Z. Jiang, and R. Surmas, 2016, Multiscale pore-network representation of heterogeneous carbonate rocks: Water Resources Research, v. 52, no. 7, p. 5433-5441, doi: 10.1002/2016WR018719.

Park, D. S., J. Upadhyay, V. Singh, K. E. Thompson, and D. E. Nikitopoulos, 2015, Fabrication of 2.5D rock-based micromodels with high resolution features: ASME Proceedings, v. 10, doi: 10.1115/IMECE2015-50657.

Peterson, G. I., M. B. Larsen, M. A. Ganter, D. W. Storti, and A. J. Boydston, 2015, 3D-printed

mechanochromic materials: ACS Applied Material Interfaces, v. 7, no. 1, p. 577-583, doi: 10.1021/am506745m.

Pham, D. T., and R. S. Gault, 1998, A comparison of rapid prototyping technologies: International Journal of Machine Tools and Manufacture, v. 38, no. 10-11, p. 1257-1287, doi: 10.1016/S0890-6955(97)00137-5.

Pilliar, R. M., M. J. Filiaggi, J. D. Wells, M. D. Grynpas, and R. A. Kandel, 2001, Porous calcium polyphosphate scaffolds for bone substitute applications - in vitro characterization: Biomaterials, v. 22, no. 9, p. 963-972, doi: 10.1016/S0142-9612(00)00261-1.

Rahman, I. A., K. Adcock, and R. J. Garwood, 2012, Virtual fossils: a new resource for science communication in paleontology: Evolution: Education and Outreach, v. 5, no. 4, p. 635-641, doi: 10.1007/s12052-012-0458-2.

Raviv, D., W. Zhao, C. McKnelly, A. Papadooulou, A. Kadambi, B. Shi, S. Hirsch, D. Dikovsky, M. Zyracki, C. Olguin, R. Raskar, and S. Tibbits, 2014, Active Printed Materials for Complex Self-Evolving Deformations: Nature: Scientific Reports, v. 4, doi: 10.1038/srep07422.

Rayna, T., L. Striukova, and J. Darlington, 2015, Co-creation and user innovation: The role of online 3D printing platforms: Journal of Engineering and Technology Management, v. 37, p. 90-102, doi: 10.1016/j.jengtecman.2015.07.002.

Reese, D., 2014, A whale of a 3D print, http://qrius.si.edu/blog/whale-3d-print, accessed August, 2016.

Reyes, R., J. A. Bellian, and D. B. Dunlap, 2008, Cyber Techniques Used to Produce Physical Geological Models: Geological Society of America Abstracts with Programs, v. 40, p. 136.

Roberson, D. A., A. R. Torrado Perez, C. M. Shemlelya, A. Rivera, E. MacDonald, and R. B. Wicker, 2015, Comparison of stress concentrator fabrication for 3D-printed polymeric izod impact test specimens: Additive Manufacturing, v. 7, p. 1-11, doi: 10.1016/j.addma.2015.05.002.

Rogers, C. I., K. Qaderi, A. T. Woolley, and G. P. Nordin, 2015, 3D printed microfluidics devices with integrated valves: Biomicrofluidics, v. 9, no. 1, p. 016501, doi: 10.1063/1.4905840.

Ryazanov, A, K. S. Sorbie, and R. van Dijke, 2014, Structure of residual oil as a function of wettability using pore-network modelling: Advances in Water Resources, v. 63, p. 11-21. doi: 10.1016/j.advwatres.2013.09.012.

Saffman, P. G., and G. Taylor, 1958, The penetration of a fluid into a porous medium or Hele-Shaw cell containing a more viscous fluid: Proceedings of the Royal Society A, v. 245, no. 1242, p. 312-329, doi: 10.1098/rspa.1958.0085.

Sasson, A., and J. C. Johnson, 2016, The 3D printing order: variability, supercenters and supply chain reconfigurations: International Journal of Physical Distribution and Logistics Management, v. 46, no. 1, p. 82-94, doi: 10.1108/IJPDLM-10-2015-0257.

Scalfani, V. F., and J. Sahib, 2013, A model for managing 3D printing services in academic libraries: Issues in Science and Technology Librarianship, no. 72. doi: 10.5062/F4XS5SB9

Schumacher, M., U. Deisigner, R. Detsch, and G. Ziegler, 2010, Indirect rapid prototyping of biphasic calcium phosphate scaffolds as bone substitutes: influence of phase composition, macroporosity and pore geometry on mechanical properties: Journal of Material Sciences, v. 21, no. 12, p. 3119-3127, doi: 10.1007/s10856-010-4166-6.

Sevenson, B., 2015, Chinese unveil mysterious 3D printed houses – built out of unique material, able to withstand devastating earthquakes: 3D Design, 3D Printing, https://3dprint.com/82322/chinese-3d-modular-homes/, accessed July, 2016.

Short, D. B., 2015, Use of 3D printing by museums: educational exhibits, artifact education and artifact restoration: 3D Printing and Additive Manufacturing, v. 2, no. 4, p, 209-215, doi: 10.1089/3dp.2015.0030.

Simon, 2015, China establishes its first national 3D printing lab for the advancement of 3D printing technologies: 3D Printer and 3D Printing News, http://www.3ders.org/articles/20150512-china-establishes-its-first-national-3d-printing-lab.html. Accessed March, 2016.

Skylar-Scott, M. A., S. Gunasekaran, and J. A., Lewis, 2016, Laser-assisted direct ink writing of planar and 3D metal architectures: Proceedings of the National Academy of Sciences of the United States of America, v. 113, no. 22, p. 6137–6142, doi: 10.1073/pnas.1525131113.

Song, W., T. W. de Haas, H. Fadaei, and D. Sinton, 2014, Chip-off-the-old-rock: the study of reservoir-relevant geological processes with real-rock micromodels: Lab on a Chip, v. 14, no. 22, p. 4382-4390, doi: 10.1039/C4LC00608A.

Sorbie, K. S., and A. Skauge, 2012, Can network modeling predict two-phase flow functions? Petrophysics, v. 53, no. 6, p. 401-409.

Stone, H. A., A. D. Stroock, and A. Ajdari, 2004, Engineering flows in small devices: Microfluidics towards a lab-on-chip: Annual Review of Fluid Mechanics, v. 36, p. 381-411, doi: 10.1146/annurev.fluid.36.050802.122124.

Sun, K., T. S. Wei, B. Y. Ahn, J. Y. Seo, S. J. Dillon, and J. A. Lewis, 2013, 3D printing of

interdigitated Li-ion microbattery architectures: Advanced Materials, v. 25, no. 33, p. 4539-4543, doi: 10.1002/adma.201301036.

Tabeling, P., 2005, Introduction to microfluidics: Oxford, OUP, 310 p.

Tapley, J., S. Leach, N. Walton, and S. H. Kajamohideen, 2016, 3D Printing: marketplace with federated access to printers: US Patent 9229674 B2, filed January 31, 2014, and issued January 5, 2016, 12 p.

Tibbits, S., C. McKnelly, C. Olguin, D. Dikovsky, and S. Hirsch, 2014, 4D Printing and Universal Transformation: Proceedings of the Association for Computer Aided Design in Architecture, p. 539-548.

Timur, A., 1969, Pulsed nuclear magnetic resonance studies of porosity, movable fluid, and permeability of sandstones: Journal of Petroleum Technology, v. 21, no. 6, p. 775-786, SPE-2045-PA.

Torrado Perez, A. R., D. A. Roberson, and R. B. Wicker, 2014, Fracture surface analysis of 3D-printed tensile specimens of novel ABS-based materials: Journal of Failure Analysis and Prevention, v. 14, no. 3, p. 343-353, doi: 10.1007/s11668-014-9803-9.

Tumbleston, J. R., D. Shirvanyants, N. Ermoshkin, R. Janusziewicz, A. R. Johnson, D. Kelly, K. Chen, R. Pinschmidt, J. P. Rolland, A. Ermoshkin, E. T. Samulski, and J. M. DeSimone, 2015, Continuous liquid interface production of 3D objects: American Association for the Advancement of Science, v. 347, no. 6228, p. 1349-1352, doi: 10.1126/science.aaa2397.

Vaezi, M., H. Seitz, and S. Yang, 2013, A review on 3D micro-additive manufacturing technologies: The International Journal of Advanced Manufacturing Technologies, v. 67, no. 5, p. 1721-1754, doi: 10.1007/s00170-012-4605-2.

Van der Land, C, R. A., Wood, K. Wu, R. van Dijke, Z. Jiang, P. W. M. Corbett, and G. D.

Couples, 2013, Modelling the permeability evolution of carbonate rocks: Marine and Petroleum Geology, v. 48, p. 1-7, doi: 10.1016/j.marpetgeo.2013.07.006.

Vlasea, M., R. Pilliar, and E. Toyserkani, 2015, Control of structural and mechanical properties in bioceramic bone substitutes via additive manufacturing layer stacking orientation: Additive Manufacturing, v. 6, p. 30-38, doi: 10.1016/j.addma.2015.03.001.

Waller, M. A., and S. E. Fawcett, 2014, Click here to print a maker movement supply chain: how invention and entrepreneurship will disrupt supply chain design: Journal of Business Logistics, v. 35, no. 2, p. 99-102, doi: 10.1111/jbl.12045.

Watson, F., S. Geiger, E. Mackay, M. Singleton, T. McGravie, T. Anouilh, D. Jobe, S. Zhang, S. Agar, S. Ishutov, F. Hasiuk, and R. C. Chalaturnyk, 2016, Comparison of flow and transport experiments on 3D-printed 'rocks' with direct numerical simulations: American Geophysical Union Fall Meeting.

West, J., and G. Kuk, 2016, The complementarity of openness: How MakerBot leveraged Thingiverse in 3D printing: Technological Forecasting and Social Change, v. 102, p. 169-181, doi: 10.1016/j.techfore.2015.07.025.

White, J. E., 1975, Computed seismic speeds and attenuation in rocks with partial gas saturation: Geophysics, v. 40, no. 2, p. 224-232, doi: 10.1190/1.1440520.

Whitesides, G. M., and A. D. Stroock, 2001, Flexible methods for microfluidics: Physics Today, v. 54, p. 42-48, doi: 10.1063/1.1387591.

Williams, W. J. W., 2013, Universal design in geoscience education: promoting student success with accessibility using local 3D printing for learner-centered instruction: Geological Society of America Abstracts with Programs, v. 45, p. 367.

Wu, H., T. W. Odom, D. T. Chiu, and G. M. Whitesides, 2003, Fabrication of complex three-

dimensional microchannel systems in PDMS: Journal of the American Chemical Society, v. 125, no. 2, p. 554-559, doi: 10.1021/ja021045y.

Yazdi, A. A., Popma, A., Wong, W., Nguyen, T., Pan, Y., and J. Xu, 2016, 3D printing: an emerging tool for novel microfluidics and lab-on-a-chip applications: Microfluidics and Nanofluidics, v. 20, no. 50, p. 1-18, doi: 10.1007/s10404-016-1715-4.

Zhang, M. J., E. Q. Li, A. A. Aguirre-Pablo, and S. T. Thoroddsen, 2016a, A simple and low-cost fully 3D-printed non-planar emulsion generator: RSC Advances, v. 6, p. 2793-2799, doi: 10.1039/c5ra23129a.

Zhang, S., H.-H. Liu, M. I. J. van Dijke, S. Geiger, and S. M. Agar, 2016b, Constitutive relations for reactive transport modeling: effects of chemical reactions on multi-phase flow properties. Transport in Porous Media, v. 114, no. 3, p. 795-814, doi: 10.1007/s11242-016-0744-5.

Zhang, S., and H.-H. Liu, 2016, Porosity–permeability relationships in modeling salt precipitation during CO_2 sequestration: Review of conceptual models and implementation in numerical simulations: International Journal of Greenhouse Gas Control, v. 52, p. 24-31, doi: 10.1016/j.ijggc.2016.06.013.

Zhao, B., MacMinn, C.W., and R. Juanes, 2016, Wettability control on multiphase flow in patterned microfluidics: Proceedings of the National Academy of Sciences of the United States of America, v. 113, no. 37, p. 10221-10448, doi: 10.1073/pnas.1603387113.

Zheng, J., L. Zheng, H.-H. Liu, and Y. Ju, 2015, Relationships between permeability, porosity and effective stress for low-permeability sedimentary rock: International Journal of Rock Mechanics and Mining Sciences, v. 78, p. 304-318, doi: 10.1016/j.ijrmms.2015.04.025.

AUTHORS

Sergey Ishutov is a Ph.D. candidate in geology at Iowa State University. He has received BSc degree in petroleum geology from the University of Aberdeen in Scotland and MSc degree from California State University in Long Beach. His research experience is in acquisition, processing, and interpretation of seismic data and analysis of computed tomography data from reservoir core plugs.

Tiffany Dawn Jobe joined the Aramco Research Center – Houston in 2013 as a Research Geologist exploring topics related to carbonate sedimentology and stratigraphy, microporosity, and state-of-the-art imaging techniques. Dawn earned her BSc degree from Tulane University, and MSc and Ph.D. degrees from the Colorado School of Mines where she studied clastic sedimentary processes and carbonate stratigraphy respectively.

Shuo Zhang is a research geologist at Aramco Research Center – Houston. He received his Ph.D. in geochemistry from the Department of Earth and Planetary Science at UC Berkeley. His research interest lies in reactive transport modeling of geological carbon storage and reservoir quality prediction of clastic and carbonate rocks.

Miguel Gonzalez received his Ph.D. in physics from the University of Florida in 2012. His doctoral thesis work was on the use Micro-Electro-Mechanical Systems (MEMS) for the study of liquid helium at low temperatures. He has been a Research Scientist at Aramco Services Company since 2014, where he does research in MEMS and microfluidic devices for oil and gas applications.

Susan Agar currently leads Geology Technology for the Aramco Research Center – Houston. She has 20+ years of experience leading research and development in the upstream. Before this she was an associate professor of geology at Northwestern University. She holds a D.Sc. from Heriot Watt University, a Ph.D. from Imperial College and an MBA from the Wharton School, University of Pennsylvania.

Franciszek J. Hasiuk received a Ph.D. (2008) in geology from the University of Michigan. He then worked at ExxonMobil until Fall 2012 when he took a position as an assistant professor at Iowa State University. He currently studies carbonate geochemistry and petrophysics as well as the application of 3D printing to petrophysical analysis of reservoir rocks at GeoFabLab.

Francesca Watson received her Ph.D. in Geophysics from Durham University in 2015. She joined Heriot-Watt University in 2015 as a post-doctoral research associate investigating new visualization techniques and numerical simulations of flow and transport in 3D printed porous media.

Sebastian Geiger is the Foundation CMG Chair for Carbonate Reservoir Simulation at the Institute of Petroleum Engineering, Head of the Carbonate Reservoir Group, and a full professor at Heriot-Watt University. He authored over 110 technical papers on topics related to carbonate reservoir modelling and simulation. Sebastian received a Ph.D. from ETH Zurich and an MSc degree from Oregon State University.

Eric Mackay is the Foundation CMG Chair for Reactive Flow Simulation at the Institute of Petroleum Engineering at Heriot-Watt University, where he has worked since 1990 and leads projects on inorganic scale management, chemical EOR and CCS. Eric holds a BSc in Physics from the University of Edinburgh and a Ph.D. in Petroleum Engineering from Heriot-Watt University.

Richard Chalaturnyk is Head of the Reservoir Geomechanics Research Group, the Foundation CMG Chair in Reservoir Geomechanics for Unconventional Resources, and the AITF Industrial Research Chair in Reservoir Geomechanics at the University of Alberta. Richard joined the University in 1997 and manages research projects on subsurface containment, high pressure/temperature experiments, CCS, and reservoir geomechanical modeling.

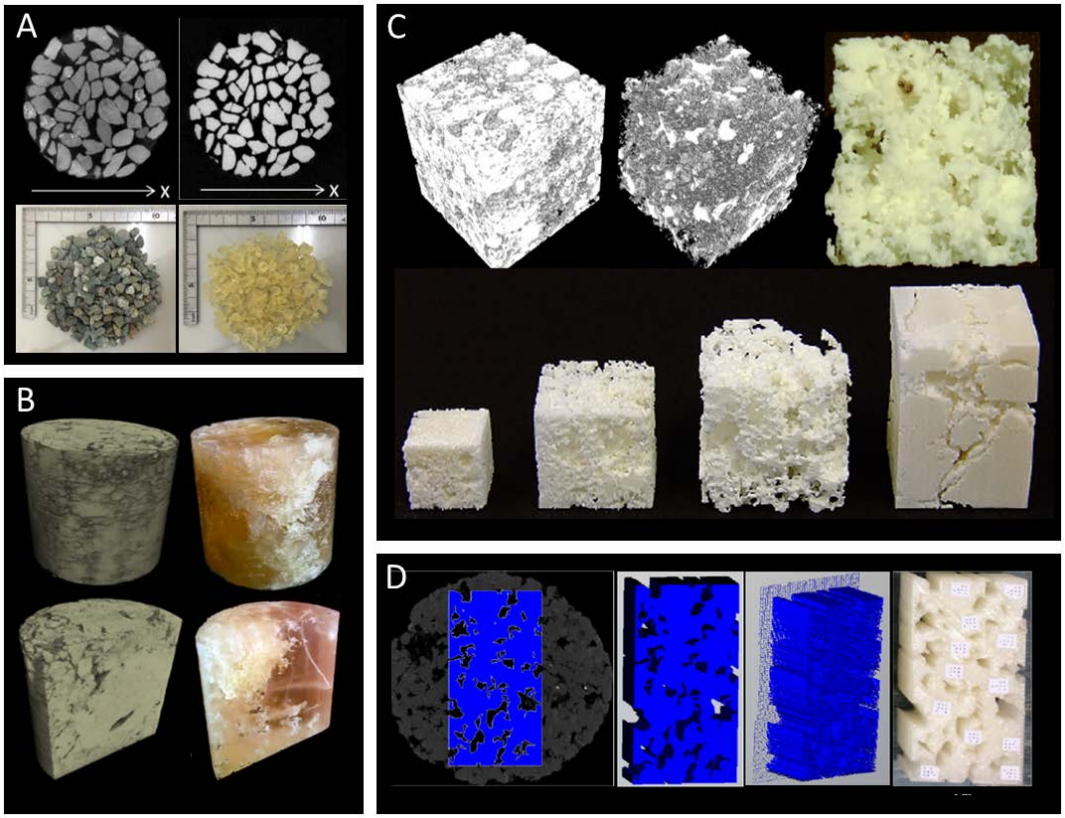

Figure 1. Selected examples of published studies using 3D printed rock proxies generated from digital models. (A) Matsumura and Mizutani (2015) 3D printed gravel material to evaluate the mechanical behavior of soil structures. Shown are X-ray micro-CT scan sections and images representing natural and 3D printed gravel. (B) Dal Ferro et al. (2015) used 3D printing to represent large undisturbed soil cores. 3D representations shown are of X-ray micro-CT scans and images of the associated 3D printed soil core. (C) Similarly, Otten et al. (2012) employed X-ray micro-tomography imaging to generate a range of 3D printed soil replicas to study soil-fungal relationships. (D) Jiang and Zhao (2015) generated 3D printed rock proxies from CAD models to study a mechanical behavior of 3D printed rock proxies.

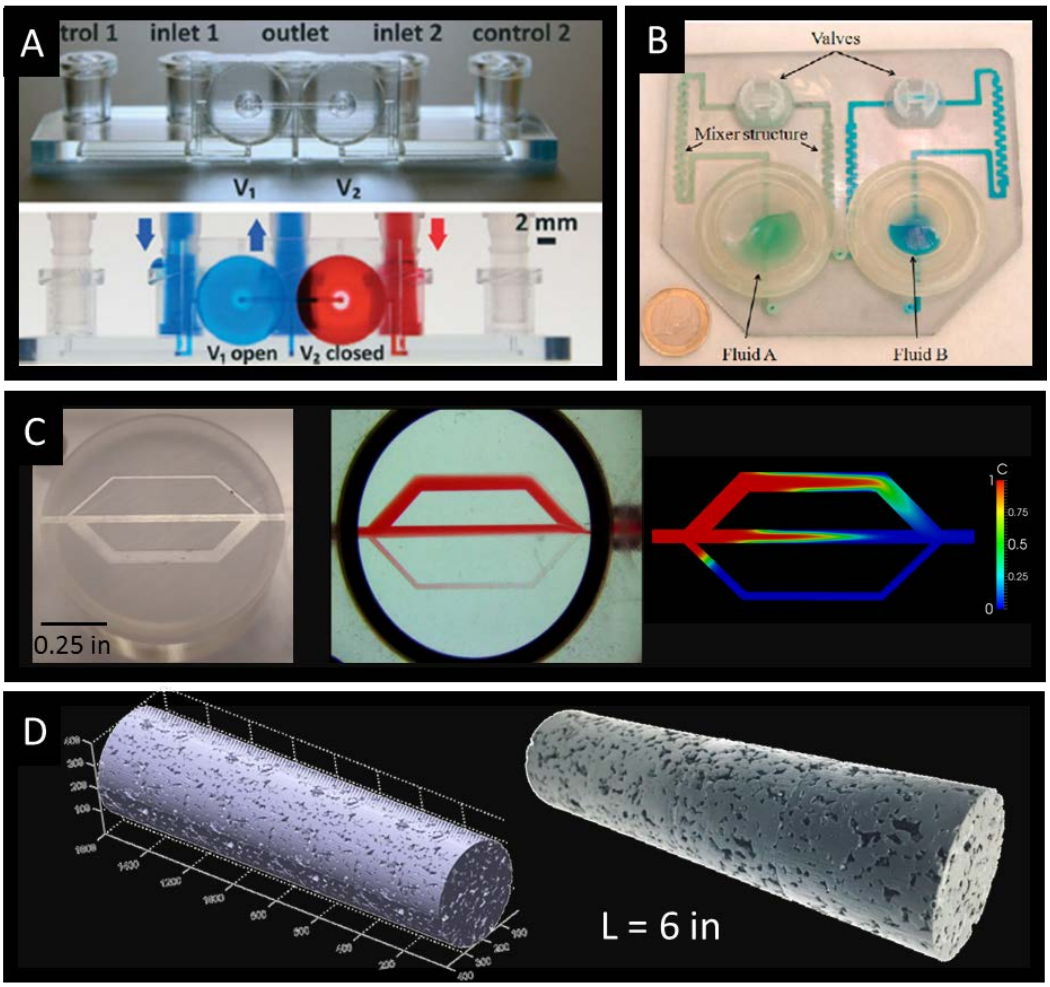

Figure 2. Selected examples of published studies using 3D printed devices and rock proxies for microfluidic and flow phenomena. (A) Yazdi et al. (2016) and (B) Bonyar et al. (2010) both show examples of translucent microfluidic devices designed for fluid mixing and homogenization for visualizing sample and reagent interactions. (C) Watson et al. (2016) demonstrated the utility of translucent 3D printed microfluidic devices for comparison of flow and transport experiments with direct numerical simulations. (D) This is an example of a 3D digital representation of a natural sandstone core plug (left) and the 3D printed rock proxy used in core flood experiments (right) at the Aramco Research Center in Houston.

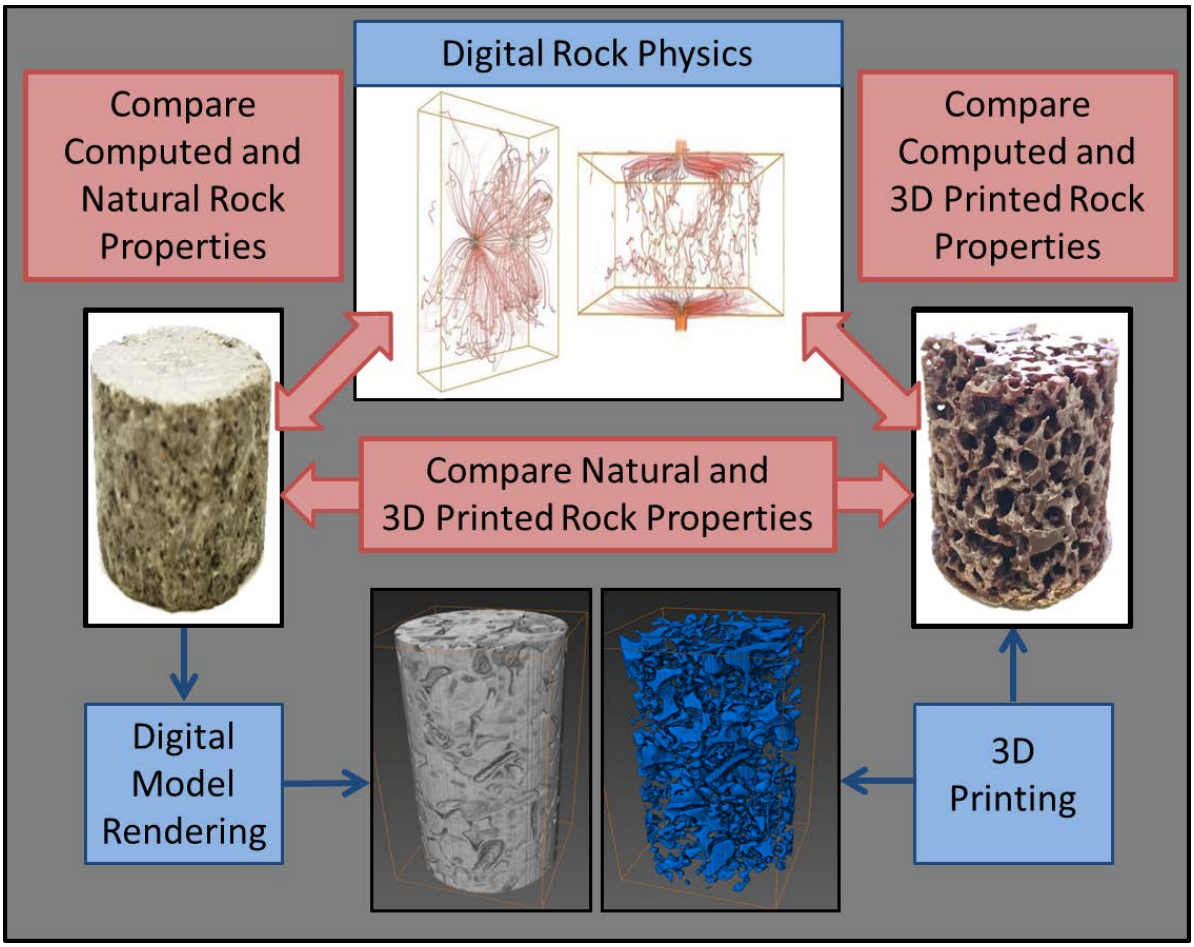

Figure 3. Workflow for comparison of macroscopic rock properties to digital models and 3D printed rock proxy properties. Macroscopic properties are defined by bulk measurements that represent a spatially averaged quantity beyond the microscopic scale and include, but are not limited to, flow (e.g., relative permeability), electrical (e.g., resistivity), acoustic (e.g., P and S wave velocities), and magnetic (e.g., NMR) properties.

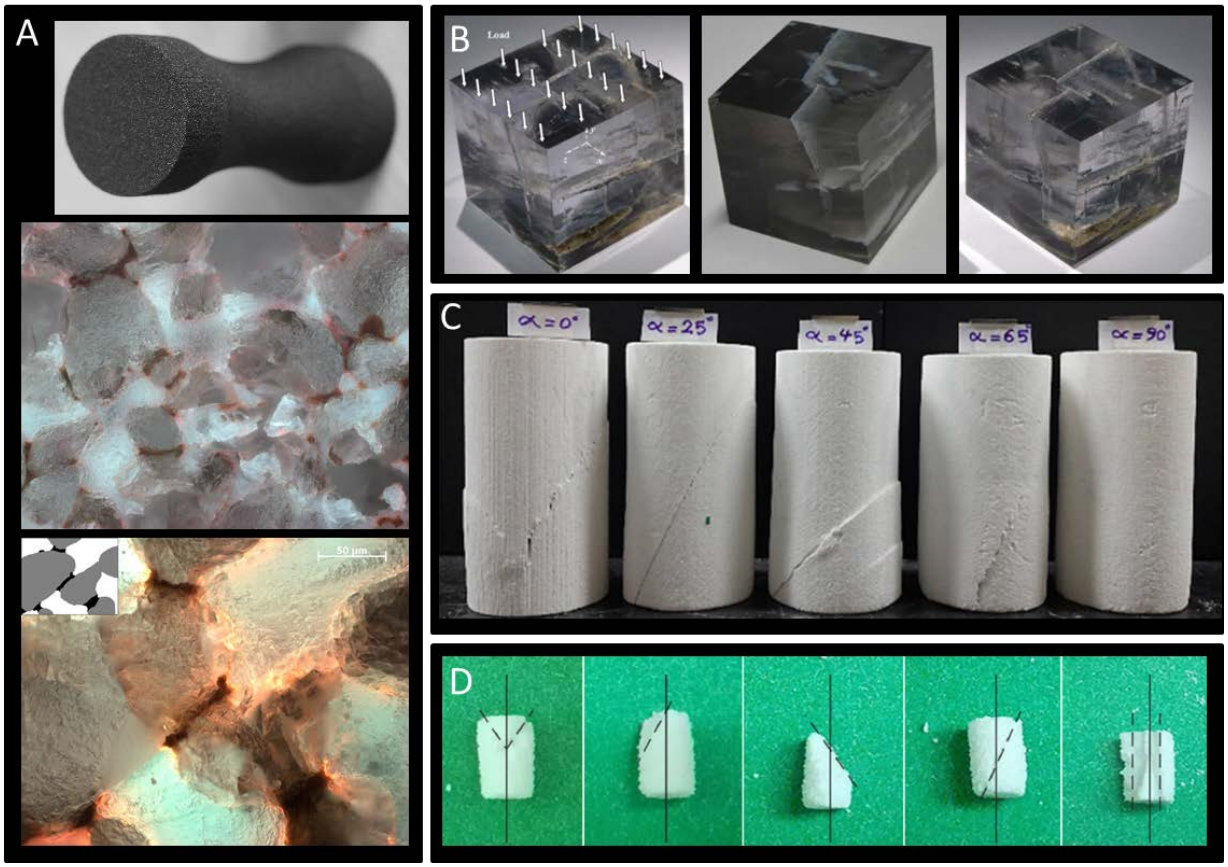

Figure 4. Applications of 3D printing to geomechanical experiments. (A) Osinga et al. (2015) manufactured proxies for uniaxial compression testing using a sand-binding 3D printer. (B) Ju et al. (2014) used 3D printing to visualize fracture geometries and associated stress concentrations in naturally occurring coal. (C) Fereshtenejad and Song (2016) tested uniaxial mechanical strength of rock proxies printed in gypsum powder. (D) Vlasea et al. (2015) explored the impact of layer orientation relative to compression direction on sample strength.

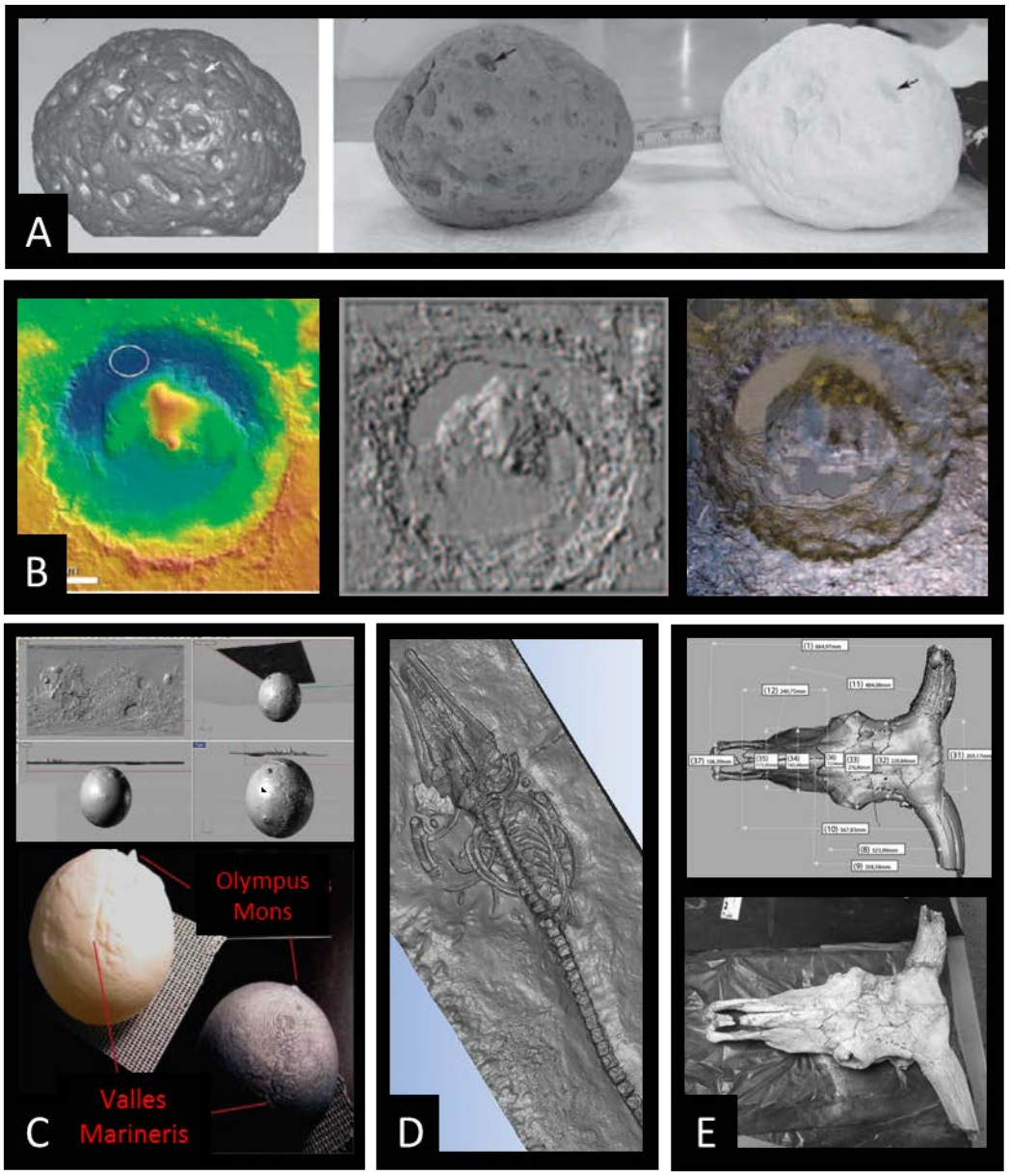

Figure 5. Examples of 3D printing applications in geomorphology and paleontology. (A) Bourke et al. (2008) generated a 3D printed rock proxy from a CAD model of a vesicular basalt clast for use in rock-breakdown experiments. Horowitz and Schulz (2012) used 3D printing to demonstrate geomorphic features on Mars, including (B) a 3D print of the Gale Crater generated from a colored topographic map and (C) several 3D models of Mars with different vertical exaggerations. (D) Byers and Woo (2015) discussed the use of 3D printing of paleontological samples from the Smithsonian digital fossil dataset. (E) Barco et al. (2010) established 3D printing as a viable technique for preservation and display of macrofossils; an example digital model and representative 3D print are shown.

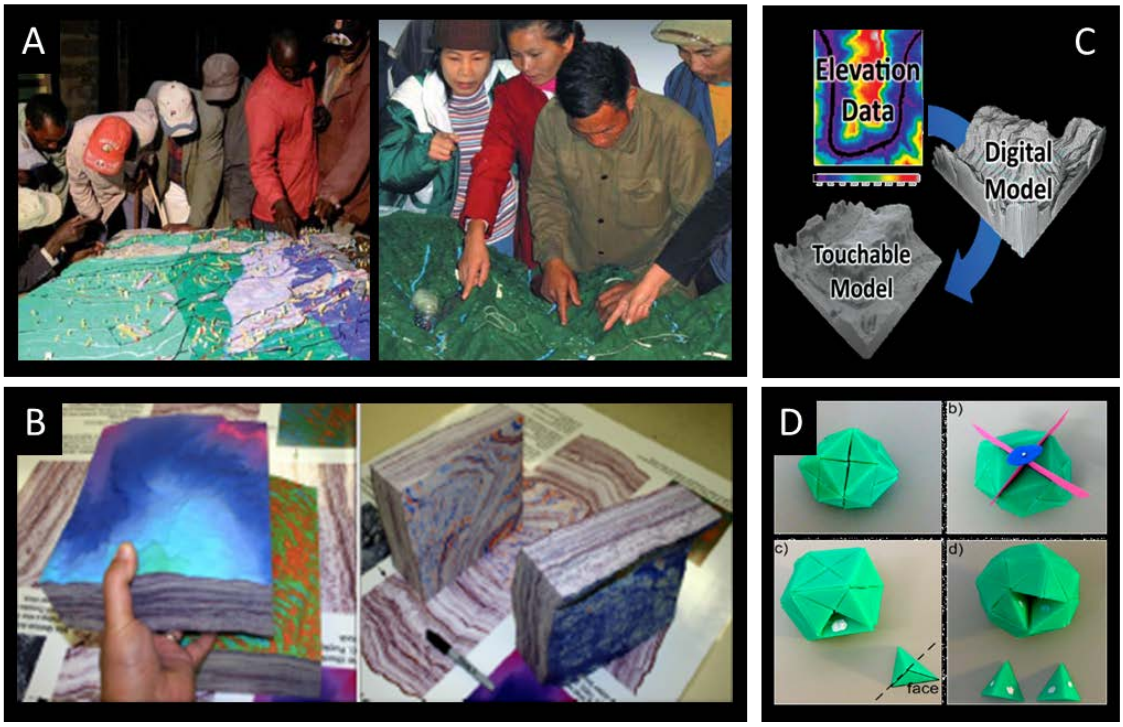

Figure 6. Examples of 3D printing applications in education and communication. (A) Ghawana and Zlatanova (2013) review 3D printing applications for urban planning, with public participation in planning using a 3D printed terrain model shown. (B) shows a 3D printed seismic volume as a way to visually enhance spatial perspective (Reyes et al., 2008). (C) Hasiuk and Harding (2016) discuss the use of 3D printing digital terrain models for use in teaching. Shown is an example workflow for printing the Grand Canyon. (D) Casas and Estop (2015) used 3D printed dissection models for teaching crystallographic concepts.

Table 1. Overview of 3D printing methods and specifications. Compiled from Pham and Gault, 1998; Camisa et al., 2014; Gao et al., 2015.

Technology	Material	Power source	Resolution (XY/Z), microns	Accuracy, microns	Maximum model dimensions, mm^3	Cost, US$x1,000	Applications in geosciences	Capabilities
ereolithography A), Digital Light ocessing (DLP)	Ceramics (alumina, zirconia), polymers, resins	Ultraviolet laser light	75/25	50	500x500x600	3-700	• Geomechanics (fracture studies) • Flow experiments on sandstones and macroporous carbonates • Geomorphology	• High building speed • Minimal to absent material microporosity
ed Depositional odeling (FDM), used Filament brication (FFF), nkjet/Polyjet	Thermoplastics, ceramic slurries, metal pastes, wax	Thermal energy	150/25	20	500x500x500	0.5-200	• Geomorphology • Flow experiments on sandstones and macroporous carbonates	• High building speed • Multi-material printing
irect Ink/Laser Writing (DIW/DLW)	Colloidal gels, suspensions, polymer melts, waxes, concentrated polyelectrolyte complexes	Thermal energy; Laser	1/0.15	0.5	85x50x25	40-3,000	• Flow experiments microporous carbonates • Microfluidic studies • Microfracture studies	• Highest resolution • Absence of material microporosity • Fastest build time
elective Laser intering (SLS)	Polymers, metals, ceramics	High-powered laser	150/50	50	330x380x425	200-750	• Scaled reservoir models built from seismic and well data	• High strength/ stiffness of 3D printed models • High accuracy • Powder recycling
elective Laser Melting (SLM)	Metal (stainless steel, Co, Cr, Ti) and ceramic powders		200/100	100	350x350x400	250-400	• Testing acoustic and electric properties of deterministic reservoir rock models	• 3D printed models have high stiffness and strength
Electron Beam Melting (EBM), lectronic Beam Welding (EBW)		Electron beam	100/100	100	200x200x100	130-1,500	• Pore scale flow experiments	• 3D printed models have high stiffness and strength

ser Engineered Net Shaping (LENS)	Molten metal powder	Laser	25/100	10	91x91x152	200-1,700	• Flow experiments on sandstones macroporous carbonates • Rock physics experiments	• Functionally graded material printing • High accuracy
minated Object Manufacturing DM), Deposition mination (SDL)	Plastic film, metallic sheet, ceramic tape, paper, polymer	Laser, Tungsten blade	10/100	200	800x550x500	12-150	• Geomorphology	• High surface finish • Low costs for supplies
Binder Jetting	Powder (silica, plaster, ceramic, metal)	Thermal energy	100/50	50	350x350x450	70-700	• Scaled reservoir models built from seismic and well data • Geomechanics (fracture studies) • Geomorphology	• Color printing • Wide material selection

4

5